DEUTSCHES ELEKTRONEN-SYNCHROTRON DESY

DESY 78/66
November 1978

QUARKONIUM

by

M. Krammer
Department of Theoretical Physics, University of Bielefeld

H. Krasemann
Deutsches Elektronen-Synchrotron DESY, Hamburg

NOTKESTRASSE 85 · 2 HAMBURG 52

To be sure that your preprints are promptly included in the
HIGH ENERGY PHYSICS INDEX ,
send them to the following address (if possible by air mail) :

DESY
Bibliothek
Notkestrasse 85
2 Hamburg 52
Germany

QUARKONIUM

by

M. Krammer [+]

Department of Theoretical Physics, University of Bielefeld

and

H. Krasemann [++]

Deutsches Elektronen-Synchrotron DESY, Hamburg

Lecture given by H. Krasemann at the Advanced Summer Institute,
Karlsruhe, September 1 - 15, 1978

+
permanent address: Deutsches Elektronen-Synchrotron DESY, Hamburg

++
present address: II.Institut für Theoretische Physik, Universität Hamburg

QUARKONIUM CONTENT

1st Lecture page

1. Introduction 2
2. The Spectrum 4
3. Spin Interactions 9
4. Scaling the Schrödinger Equation 13

2nd Lecture

5. Radiation 21
   a) Electric Dipole Radiation 21
   b) E1 Sum Rules 23
   c) Magnetic Dipole Radiation 28
   d) Scaling of E1 and M1 28
   e) Problems with M1 in Charmonium 29
   f) Gluon Radiation 31
6. Annihilation 32
   a) Annihilation Formulae 32
   b) Ratios and Applications 37
7. Jets 40
8. Conclusions 49

1. Introduction

Since the discovery of the J/Ψ and Ψ' in November 1974 [1] we all witnessed a dramatic revival of the quark model [2]. A new quark flavour, c = charm [3], was added to the hadron spectroscopy, interpreting the J/Ψ and Ψ' as $c\bar{c}$ bound states. This new system promised to be describable as nonrelativistic bound states of c and $\bar{c}$: Charmonium [4]. While the quark model for old mesons suffered from the fact that the quarks move relativistically (mass differences of old mesons are of the order of the masses themselves), in charmonium the relatively heavy (≈ 1.5 GeV) c-quarks should move relatively slowly, $\beta^2 = (v/c)^2 \approx 0.2$. A perturbation expansion in β^2 then converges rapidly and the well known powerful tools of exploring a nonrelativistic bound system could be used. This was the source of real excitement.

Meanwhile we learned about the existence of a still heavier meson family, the Υ, Υ' and Υ'' [5], and interpret it as bound states of the b quark and $\bar{b}$, b being the fifth quark flavour [6], much more massive than charm. We further hope to discover the sixth quark flavour, t maybe, and its bound states $t\bar{t}$ in the new e^+e^- machines PETRA and PEP. The larger masses of the b and t quark guarantee that their bound systems $b\bar{b}$ and $t\bar{t}$ are nonrelativistic to a much higher degree than $c\bar{c}$. In this lecture we will discuss the dynamics of a nonrelativistic $Q\bar{Q}$ bound system, Q = c,b,t. As a title for this lecture we chose the generic name for a nonrelativistic $Q\bar{Q}$ system, QUARKONIUM.

On the field theory side, Quantumchromodynamics [7], QCD, turned out to be the most promising key to an understanding of quark dynamics. QCD is a nonabelian gauge field theory of the interactions of quarks and eight massless vector gauge bosons, the gluons. The coupling constant α_s , renormalized at the relevant momentum transfer q^2 or the corresponding distance R, turns out to be a monotonously falling function of q^2 (or rising function of R). It tends logarithmically to zero as $q^2 \longrightarrow \infty$ or $R \longrightarrow 0$, this is called asymptotic freedom [8]. α_s becomes large for some large R of the order of one fm, the typical hadron size. Up to today this regime is subject to speculations only, we believe that the rising coupling provides for the permanent confinement of quarks. Perturbation theory is useless in this

case, but lattice gauge theories [9] or the string model [10] suggest that the interquark force for large separations might be independent of the distance, thus giving rise to a linearly rising static potential between quarks. At short distances physics is much more pleasant because α_s becomes small. Then perturbation theory is fine and in Born approximation the quark interaction is just one gluon exchange. The nonabelian self-interaction of the colour-charged gluons plays no rôle in lowest order graphs, and in this approximation gluons are just analogous to photons. The short distance behaviour of QCD is thus very similar to QED, the static potential for short distances being of the Coulomb type.

When QCD is in fact the underlying theory for the Quarkonium systems, we should be able to probe some QCD features by studying these systems. What can we probe? First we should be able to probe the short distance behaviour. The one gluon exchange at short distances leads to a static potential of the form $V_{AF}(R) = -\frac{4}{3}\frac{\alpha_s}{R}$. The subscript AF denotes the origin of this potential "Asymptotic Freedom". -4/3 is a group factor from SU3 (colour) and α_s is the effective coupling. One can take two points of view regarding α_s . Either α_s is really R-dependent [11] but independent of the quark flavour. Or one defines an effective α_s as a constant, different for each quark flavour mass [8]. For simplicity we take the second point of view. Then the α_s in a heavy $Q\bar{Q}$ bound state M_2 is related to that of a lighter one M_1 by the approximate formula

$$\alpha_s(M_2^2) = \alpha_s(M_1^2)\left[1 - \frac{33-2N}{12\pi}\alpha_s(M_1^2)\log(M_1^2/M_2^2)\right]^{-1} \qquad (1.1)$$

(N is the number of "light" (= lighter than Q) quarks). The potential $V_{AF}(R)$ with α_s given by (1.1) should be correct for very short distances. It further gives rise to the spin-spin and spin-orbit interactions known from positronium, because the quark gluon vertex has the same Dirac structure as the electron photon vertex (γ_μ-coupling).

The second feature of QCD we might be able to probe is the large distance behaviour, $R \longrightarrow \infty$. The linear potential as suggested by lattice gauge theory or string models should dominate for very large distances R:

$V_C(R) = \alpha \cdot R$. The subscript C stands for "Confinement". The slope α should be flavour independent and also somehow related to the inverse Regge slope of the low mass mesons [12]. Furthermore this potential should be essentially spin independent [9].

We now have guesses for the static potential at very short distances, $V_{AF}(R) = -\frac{4}{3}\frac{\alpha_s}{R}$, and very long distances $V_C(R) = aR$. We have no guess for intermediate distances. The simplest assumption is to write the complete potential as a superposition of these two extremes(E.Eichten et al.,ref.4):

$$V(R) = V_{AF}(R) + V_C(R) \tag{1.2}$$

We further assume that all the spin dependence (except the kinematic Thomas precession) has its origin in $V_{AF}(R)$ and can be calculated via the Fermi-Breit Hamiltonian [13]. Although these Ansätze have their criticism they have worked out to be very useful as a first attempt to the problem. The first part of this lecture will try to show how far these Ansätze reach. In the second part we will discuss decays of Quarkonium and a third test of QCD, namely of gluon helicities and the gluon self coupling. With the experimentally accessible regime of c.m. energies of 10 GeV or more, the gluons which govern annihilations in QCD, might show up as hadron jets [14]. These jets should carry the directed momentum of the initial gluon. In angular distributions of these jets one should then be able to measure gluon helicities [14,15]. One can further speculate on the existence of glueballs [16] to be found in Quarkonium decays and on measuring the nonabelian gluon self coupling by comparing the angular distribution of a 3 gluon decay versus a γ + 2 gluon decay. The latter two things, however, go beyond the Born approximation.

2. The Spectrum

Throughout the discussion we will assume that the Quarkonium ($Q\bar{Q}$) system is essentially nonrelativistic. The perturbative Hamiltonian can then be obtained by solving the Bethe Salpeter equation in nonrelativistic approximation or by expanding the exact relativistic scattering amplitude (Born graph only). One obtains the Schrödinger equation in zeroth order of β^2 and the well known Fermi-Breit Hamiltonian terms up to order β^2 . In

0th order

$$H^{\circ} = 2 m_Q + \frac{\vec{p}^{\,2}}{m_Q} + V(R) + \text{const.} \qquad (2.1)$$

and all states which only differ in their quark spin configurations are degenerate.

Here we can study the rough structure of the spectrum and try to justify the choice (1.2) for the potential V(R.). In Fig. 2.1 it is demonstrated

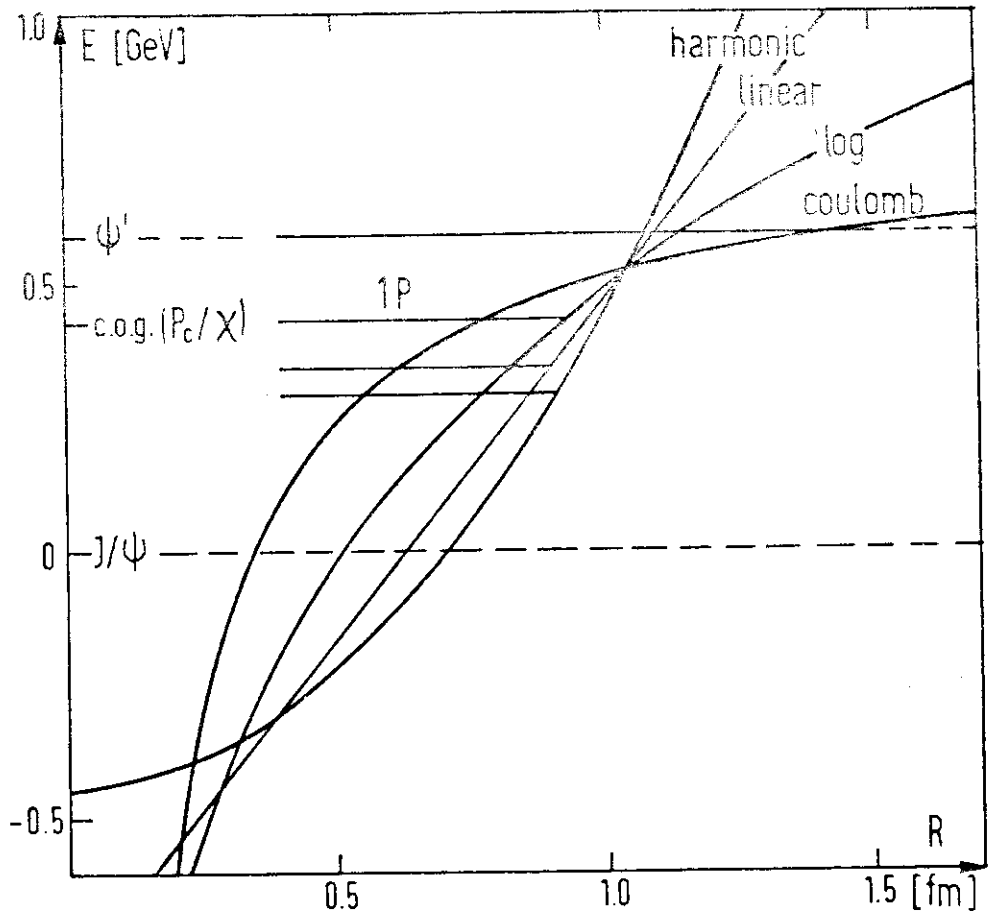

Fig. 2.1. Four different potentials for charmonium, normalized to the J/Ψ and Ψ′ binding energies. The solid horizontal lines indicate the P wave of each potential, the experimental c.o.g.(P) is given for comparison.

that the center of gravity of the P waves (which is object of 2.1) can be well described if the potential lies between a Coulombic and a linear potential. Also a logarithmic potential is not bad. This may serve to justify the Ansatz (1.2). We note, however, that doing this comparison we assume that splittings due to spin-spin interactions are either small or of the same magnitude in the P and S waves. Calculations of the spectrum of Eq. (2.1) have to be done numerically because of the complicated nature of the potential V(R). There are three parameters, m_Q, $\kappa \equiv \frac{4}{3}\alpha_s$ and a. The level splitting of the radial excitation and the ground state ($\Psi'(3.7)$ and J/Ψ (3.1) in Charmonium) determines one of the potential parameters, say a, if the other, say κ, is given. We then can try to determine κ from two independent sources, namely the ratio of the S wave functions at the origin

$$\frac{|\Psi_{\Psi'}(0)|^2}{|\Psi_{J/\Psi}(0)|^2} = \frac{M_{\Psi'}^2 \Gamma_{e\bar{e}}(\Psi')}{M_{J/\Psi}^2 \Gamma_{e\bar{e}}(J/\Psi)} = \frac{(3.7)^2 \cdot 2.2\ \text{keV}}{(3.1)^2\ 4.8\ \text{keV}} \tag{2.2}$$

and the relative placement of the center of gravity of the P waves. Both procedures are almost independent of the third parameter, m_Q, and in Charmonium they give

$$\begin{aligned} \kappa &= 0.4 \ldots 0.5 \\ a &= 1 \ldots 0.9\ \text{GeV/fm} \end{aligned} \tag{2.3}$$

One remark on Eq. (2.2) is in order. It is derived from the Van Royen-Weisskopf formula

$$\Gamma_{e\bar{e}}(V) = 16\pi\alpha^2 e_Q^2 \frac{|\Psi_V(0)|^2}{M_V^2} \tag{2.4}$$

This equation is subject to large corrections in the Charmonium system as we will discuss later but in ratios of $\Gamma_{e\bar{e}}$'s these corrections cancel. Therefore (2.2) seems to be quite reliable.

Is the large value of κ reasonable? From the beginning κ is just a free parameter. But with $\kappa = 4/3\,\alpha_s$ we find α_s of the magnitude 0.3 ... 0.4. Is this α_s related to the strong coupling constant in annihilation processes? Or is it related to the strong coupling constant in deep inelastic lepton scattering? From the decay formulae as described in the second lecture one can derive α_s(annihilation at 3 GeV) $\simeq$ 0.2. But this α_s refers to annihilation distances which are shorter than the average interquark distances. From deep inelastic lepton scattering we find $\alpha_s(3\ \text{GeV}) \simeq \alpha_s(0.07\ \text{fm}) \simeq 0.4$ taking the renormalization point λ = 0.5 GeV, as you have learned in this school [17]. From Fig. 2.2 we see

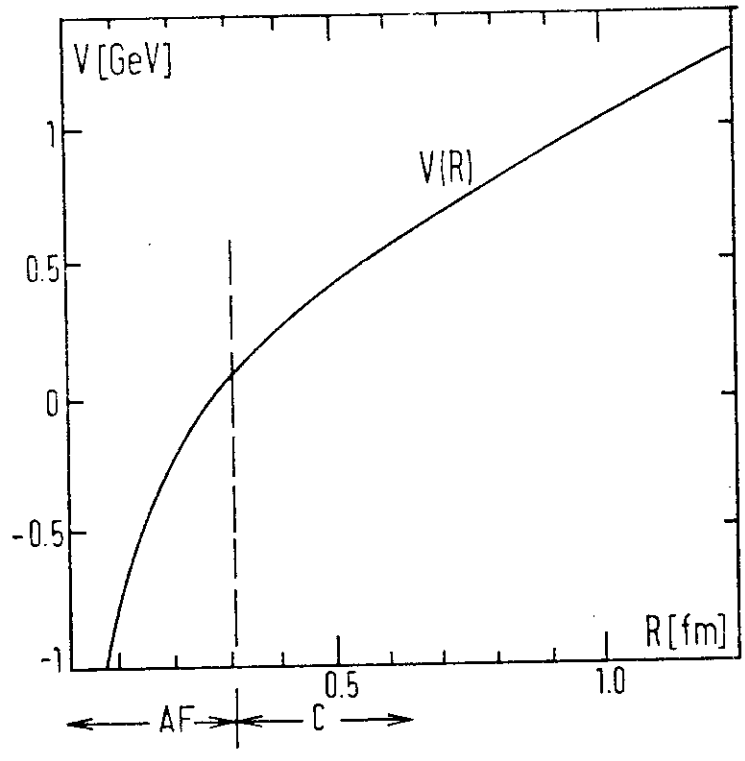

Fig. 2.2. The shape of the standard potential, eq. (1.2). V_{AF} dominates below, V_c above R = 0.3 fm.

that 0.07 fm are just in the middle of the range where the asymptotic freedom potential V_{AF} dominates, between 0 and 0.3 fm. The α_s as determined from the spectrum with the simple Ansatz (1.2) for V(R) agrees roughly with the α_s as measured in scaling violations of deep inelastic lepton scattering. This result encourages us to ask the next question: Is the parameter α in $V_c(R) = aR$ unique for all flavours (quark masses) as QCD suggests?

The first estimates of the V'-V splittings in $Q\bar{Q}$ systems heavier than Charmonium predicted a decrease of this splitting with m_Q [18]. At 10 GeV the mass splitting should be 450 MeV only (compared to 590 MeV in Charmonium). As soon as the next Quarkonium system, Υ and Υ', was found, this prediction was destroyed. The $\Upsilon'-\Upsilon$ mass splitting was around 600 MeV again as in Charmonium. The potential to describe this fact is the logarithmic potential [19]. Here mass splittings are completely independent of the quark mass. But an overall log potential has no justification within QCD. For intermediate distances, on the other hand, it is not worse than the simple superposition (1.2). An interesting - and phenomenologically successful Ansatz was then proposed with the log potential for <u>intermediate</u> distances only [20]:

$$V(R) = \begin{cases} -\kappa/R & R < R_1 \\ b \cdot \log R/R_0 \quad \text{for} & R_1 \leq R \leq R_2 \\ \alpha \cdot R & R > R_2 \end{cases} \tag{2.5}$$

The ambiguities coming in by 6 parameters, κ, a, R_1, R_2, R_0, b in this potential are removed by demanding V(R) to be continuously differentiable at R_1 and R_2. These are four conditions which remove 4 parameters and for comparison one chooses κ and a to be the only independent potential parameters. The Charmonium system has been solved with this potential and one finds a very good fit to all available data with

$$\frac{3}{4}\kappa = \alpha_s = 0.31$$
$$\alpha = 0.775 \ \text{GeV fm}^{-1} \tag{2.6}$$

Applying the potential (2.5) - with the unique a = 0.775 GeV/fm - to the Υ system gives the mass difference $\Upsilon' - \Upsilon$ to 560 MeV.

Very recently a precise measurement of the Υ and Υ' masses at DORIS gave us the experimental value: 560 MeV [5]. This coincidence is of course no prove for the correctness of the potential (2.5) but it shows that - with

a more sophisticated potential - the assumption of a flavour independent constant force between quarks at long distances is not in contradiction with what we observe. It is amusing to note that this value of a = 0.775GeV/fm is even in agreement with what one would expect from the old meson spectroscopy [12].

We want to add a remark on quark masses. Quark masses only slightly influence the two inputs we used, the ratio of wave functions at the origin and the P wave location. What they mainly influence is the wave functions themselves, the dipole matrix elements and the velocity of the quarks. But here is some ambiguity. Fitting $\Psi(o)$ to the naive V. Royen Weisskopf formula (2.4) gives a rather small value, $m_c \simeq 1.1$ GeV. For the dipole matrix elements on the other hand one would like a large quark mass, $m_c \simeq 2$ GeV. In the best known studies at Cornell [21] the requirement of small quark velocities restricts m_c to be $m_c \simeq 1.6$ GeV. To fix m_c or m_Q resp. is not as easy as to fix α_s and a, because the decay formulae (2.4) and the dipole formula are subject to large corrections as we will discuss in the second lecture. We will use scaling arguments for scale variations of the quark mass. To overcome the ambiguities of determining the quark masses we will set quark mass ratios equal to the corresponding bound state mass ratios. We emphasize that smaller quark masses like $m_c = 1.1$ GeV do not destroy the nonrelativistic approximation. We have calculated $\beta^2 = (v/c)^2$ and find that $\beta^2 < 0.3$ in J/Ψ and $\beta^2 < 0.4$ in Ψ' for $m_c = 1.16$ GeV and $\kappa < 0.55$. We feel that this justifies to leave the quark masses themselves an open question.

3. Spin Interactions

In the physical charmonium spectrum the Schrödinger states are split up due to spin interactions. In this chapter we want to compare the magnitude of these splittings with the simplest Ansatz we can imagine, the Fermi Breit Hamiltonian.[13] These higher order corrections to (2.1) are relativistic kinematic corrections and spin corrections:

$$H = H^0 + H^{rel} + H^{spin} \tag{3.1}$$

The spin corrections have three contributions.

$$\text{spin orbit:} \quad H^{LS} = \frac{2}{m_Q^2}\,\vec{L}\cdot\vec{S}\left[\frac{1}{R}d_R\right]\left(V_{AF}(R) - \frac{1}{4}V(R)\right)$$

$$\text{tensor:} \quad H^{T} = \frac{-1}{12\,m_Q^2}\left(3\,\vec{\sigma}_1\cdot\hat{R}\,\vec{\sigma}_2\cdot\hat{R} - \vec{\sigma}_1\cdot\vec{\sigma}_2\right)\left[d_R^2 - \frac{1}{R}d_R\right]V_{AF}(R) \qquad (3.2)$$

$$\text{spin-spin:} \quad H^{SS} = \frac{1}{6\,m_Q^2}\,\vec{\sigma}_1\cdot\vec{\sigma}_2\;\Delta V_{AF}(R)$$

Here $\vec{\sigma}_i/2$ is the quark spin, $S = 1/2(\vec{\sigma}_1 + \vec{\sigma}_2)$ the meson spin, $\vec{L}$ its angular momentum, $\vec{R}$ the interquark distance. For the potential V(R) we again take the simplest Ansatz (1.2) with only $V_{AF}(R)$ being spin-dependent. As mentioned in the introduction lattice gauge theories suggest that the confinement part $V_c(R)$ of the potential is spin-independent. Nevertheless it contributes to the spin orbit interaction due to the relativistic kinematic effect of the Thomas precession [22], $-1/4V(R)$ in H^{LS}. In Quarkonia the Thomas precession leads to a decrease of the $^3P_2$ - $^3P_1$ splitting relative to the $^3P_1$ - $^3P_0$ splitting. While in Positronium, where $V(R) \sim -1/R \sim V_{AF}(R)$

$$\frac{M(^3P_2) - M(^3P_1)}{M(^3P_1) - M(^3P_0)} = 0.8 \qquad (3.3)$$

the additional $V_c(R)$ in the interquark potential (1.2) leads to a decrease of (3.3), which experimentally is found to be 0.5 in Charmonium.

We are confident that the Fermi Breit Hamiltonian (3.2) is not a too bad approximation. As an example let us consider the part of the relativistic corrections due to the kinetic energy of the quarks. This correction is $\langle (\vec{p}^2)^2/4m_Q^3 \rangle \approx E_{kin} \langle \frac{1}{4}\beta^2 \rangle$. Up to β^2 of 0.4 the relativistic kinetic energy correction is less than 10 %. The β^2 one obtains in the Charmonium calculations are 0.2 to 0.3 for J/Ψ and 0.27 to 0.4 for Ψ' varying m_c from 1.6 to 1.16 GeV.

Let us now compare experiment with the predictions from (3.2). We start considering the experimental states as discussed at this school [23]. The three P waves are quite well established, the $\chi(3.55)$ as $j^{PC} = 2^{++}$ state, the $P_c/\chi(3.51)$ as $j^{PC} = 1^{++}$ state and the $\chi(3.41)$ as $j^{PC} = 0^{++}$ state. For

the pseudoscalar partners of J/Ψ and Ψ' the experimental situation is not so clear. Candidates for the pseudoscalars are $X(2.83)$, $\chi(3.45)$ and $\chi(3.59$ or $3.18)$.

The P wave splittings can be parametrized as

$$\langle H^{LS} \rangle = A \langle \vec{L} \cdot \vec{S} \rangle$$
$$\langle H^{T} \rangle = B \langle T \rangle \qquad (3.4)$$

where the tensor operator $T \equiv 3\, \vec{\sigma}_1 \cdot \hat{R}\, \vec{\sigma}_2 \cdot \hat{R} - \vec{\sigma}_1 \cdot \vec{\sigma}_2$. The expectation values of $\vec{L} \cdot \vec{S}$ and $\vec{T}$ can be found in textbooks on Quantum mechanics [24]. For P waves they are displayed in Table 3.1. A Charmonium analysis with the

j	$\langle \vec{L} \cdot \vec{S} \rangle$	$\langle T \rangle$
2	+ 1	- 2/5
1	- 1	+ 2
0	- 2	- 4

Table 3.1

State	$^3P_2$	$^3P_1$	$^3P_0$	center of gravity
mass [GeV]	3.552	3.508	3.415	3.522

Table 3.2

experimental masses of Table 3.2 yields for A and B

$$A \simeq 34 \text{ MeV}, \qquad B \simeq 10 \text{ MeV} \qquad (3.5)$$

On the theoretical side we read off (3.2)

$$A = \frac{2}{m_Q^2} \left\langle \frac{1}{R} d_R \left(V_{AF}(R) - \frac{1}{4} V(R) \right) \right\rangle$$
$$B = \frac{-1}{12 m_Q^2} \left\langle \left(d_R^2 - \frac{1}{R} d_R \right) V_{AF}(R) \right\rangle \qquad (3.6)$$

including the Thomas precession. With our standard potential (1.2) this gives

$$A = \frac{2}{m_Q^2} \langle \alpha_s R^{-3} - \frac{1}{4} \alpha R^{-1} \rangle$$
$$B = \frac{1}{3 m_Q^2} \langle \alpha_s R^{-3} \rangle \qquad (3.7)$$

We see that the spin dependence from the one gluon exchange (V_{AF}) is governed by $\langle R^{-3} \rangle$ while the Thomas precession is governed by $\langle R^{-1} \rangle$. Taking our $\alpha_s = 0.4$, $m_c^{-1} \langle R^{-3} \rangle \simeq 0.07$ GeV^2 and $\langle R^{-1} \rangle \simeq 0.4$ GeV from numerical fits yields the values of A and B given in Table 3.3 for two different values

m_c [GeV]	1.6	1.1
A [MeV]	35-12	56-32
B [MeV]	6	9

Table 3.3: A and B from numerical fits. In row A the second number is the contribution from the Thomas precession.

of m_c [+]. By comparison of Table 3.3 with eq. (3.5) we see that we are in the right ball park. We could not have expected a better agreement from our crude approximation!

Let us now try the spin-spin interaction. According to our philosophy it arises from the short range one gluon exchange (V_{AF}) alone. The relevant term in the Fermi-Breit-Hamiltonian (3.2) was

---

[+] The tensor operator T of eq. (3.4) possesses off diagonal matrix elements, too. They lead to an S-D mixing. Two physical Charmonium states would e.g. be $\Psi'(3.7) = \sqrt{1-\varepsilon^2}\, 2^3S_1 + \varepsilon\, 1^3D_1$ and $\Psi''(3.77) = -\varepsilon\, 2^3S_1 + \sqrt{1-\varepsilon^2}\, 1^3D_1$ with $\varepsilon = \frac{2\sqrt{2}\,\alpha_s}{3 m_Q^2} \langle 2^3S_1 | R^{-3} | 1^3D_1 \rangle$ 32). With $\langle 2^3S_1 | R^{-3} | 1^3D_1 \rangle \approx \langle 1^3P | R^{-3} | 1^3P \rangle$ we can evaluate $\varepsilon \simeq 0.3$ leading to a $\Gamma_{e\bar{e}}(\Psi'(3.77))$ of 10 % of that of $\Psi'(3.7)$. Experimentally it is 17 %.

$$H^{SS} = \frac{1}{6m_Q^2}\ \vec{\sigma}_1 \cdot \vec{\sigma}_2\ \Delta V_{AF}(R) \tag{3.8}$$

The eigenvalues of the operator $\vec{\sigma}_1 \cdot \vec{\sigma}_2 = 2\vec{S}^2 - 3$ are +1 in a spin triplet state and -3 in a spin singlet state. Because $\Delta V_{AF}(R) \sim \Delta\left(\frac{-1}{R}\right) = 4\pi\,\delta(R)$ the integral over the wave functions becomes trivial and we have

$$\langle H^{SS} \rangle = \frac{4}{3}\alpha_s \cdot 4\pi \cdot \frac{1}{6m_Q^2}\,(2\vec{S}^2 - 3)\,|\psi(0)|^2 \tag{3.9}$$

Taking $|\psi(0)|^2$ from $\Gamma_{e\bar{e}}$ via eq. (2.4) and α_s from eq. (2.3) gives us for the splittings

$$\begin{aligned} M(1^3S_1) - M(1^1S_0) &\simeq 70\ \text{MeV} \\ M(2^3S_1) - M(2^1S_0) &\simeq 35\ \text{MeV} \end{aligned} \tag{3.10}$$

Trying to identify $\eta_c(1^1S_0) \equiv X(2.83)$ means 70 MeV ≡ 250 MeV, $\eta_c'(2^1S_0) \equiv \chi(3.45)$ means 35 MeV ≡ 230 MeV, or $\eta_c'(2^1S_0) \equiv \chi(3.59)$ means 35 MeV ≡ 80 MeV. Many solutions have been proposed to solve this puzzle, among these are instanton effects [25] and an anomalous colour magnetic moment of the c-quark.[26] The simplest solution might be that the $|\psi(0)|^2$ in eq. (2.4) and in (3.9) are different objects. The next order correction to $|\psi(0)|^2$ in (2.4) comes in through a transverse gluon exchange between the two quark lines before annihilation . It has a large factor in front and the total correction is a factor $\left(1 - \frac{16}{3}\frac{\alpha_s}{\pi}\right)$ [27], which in no case is small. But before continuing this discussion let us wait for estimates of some decay rates involving the pseudoscalars. Then we will find that we have much more severe problems which question the identifications above.

4. Scaling the Schrödinger Equation

The radial form of the Schrödinger equation reads

$$\left[-d_R^2 + \frac{\ell(\ell+1)}{R^2} + 2m\left(V(R) - E\right)\right] \mathcal{Q}(R) = 0 \tag{4.1}$$

For all potentials of the form

$$V(R) = a \cdot R^{\varepsilon} \quad , \quad \varepsilon > -2 \tag{4.2}$$

we can bring it into the dimensionless form

$$\left[-d_\rho^2 + \frac{\ell(\ell+1)}{\rho^2} + \rho^{\varepsilon} - \xi \right] R(\rho) = 0 \tag{4.3}$$

with the substitutions

$$\begin{aligned} \xi &= E \cdot (2m)(2ma)^{-2/(2+\varepsilon)} \\ \rho &= R \cdot (2ma)^{+1/(2+\varepsilon)} \end{aligned} \tag{4.4}$$

One can now immediately read off the scaling laws for E and R:

$$\begin{aligned} E &\sim m^{-\varepsilon/(2+\varepsilon)} \\ R &\sim m^{-1/(2+\varepsilon)} \end{aligned} \tag{4.5}$$

(4.5) is also applicable for $\varepsilon = 0$, in which case the potential is $V(R) = a \log R/R_0$. We leave the derivation to the reader.

Let us now consider some aspects of scaling for Quarkonia. We begin with the level spacing. In a potential like $V_{AF}(R) = -\frac{4}{3}\frac{\alpha_s}{R}$ alone level spacings scale like $\Delta E \sim \alpha_s^2 m_Q$, in a linear potential like $V_c(R) = aR$ they scale like $\Delta E \sim m_Q^{-1/3}$. To estimate the intermediate scaling behaviour in the standard potential we try a very crude approximation: Let us consider the level spacings given by the linear potential with the Coulombic part $V_{AF}(R)$ as a first order perturbation. Then

$$E_n = E_n(V_c) + \langle n \mid -\frac{4}{3}\frac{\alpha_s}{R} \mid n \rangle \tag{4.6}$$

and ΔE scales like $m_Q^{-1/3}$ with a first order correction $\sim \alpha_s m_Q^{+1/3}$ Because of the mass dependence of α_s , eq. (1.1), this perturbation procedure starts to break down not before $m_Q \gtrsim 100$ GeV. The curve is shown in Fig. 4.1 (dashed line). Asymptotically the states fall into

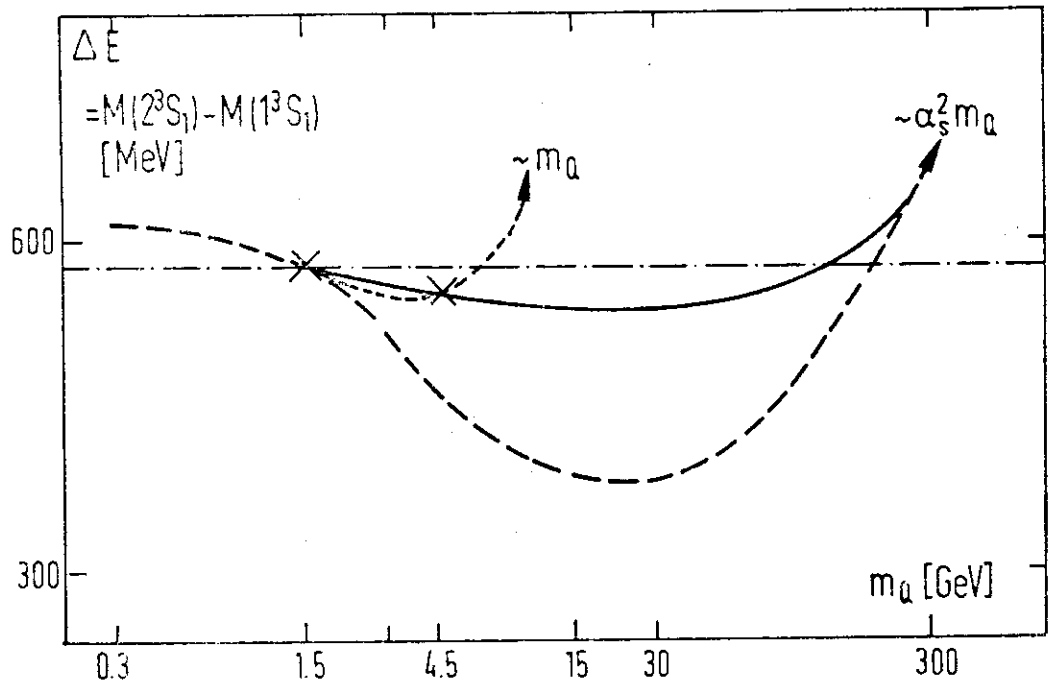

Fig. 4.1. The scaling behaviour of ΔE in different potentials.

— — — — standard potential with $\alpha_s(M^2)$ via eq. (1.1)

---------- standard potential with fixed α_s

— · — · — · logarithmic potential

———————— our guess

the Coulombic potential V_{AF} and the scaling law becomes $\Delta E \sim \alpha_s^2 m_Q$ If α_s would be a universal constant, this would happen much earlier (dotted line in Fig. 4.1). From the $\Upsilon' - \Upsilon$ mass difference we know that the simple standard potential is not adopted by nature. Using the $\psi' - J/\psi$ mass difference as input, the standard model prediction for the $\Upsilon' - \Upsilon$ mass difference is much lower than the experimental one (Fig. 4.1). The prediction can be raised to the experimental value by fixing α_s to its Charmonium value everywhere, but this seems not appealing theoretically. In Ch. 2 we saw that a reasonable description of the $\Upsilon' - \Upsilon$ mass difference was possible by introducing a logarithmic potential for intermediate distances. In the log potential ΔE = constant ($\mathcal{E} = 0$), and an intermediate part

in the potential would tend to fill up the valley of the dashed curve in Fig. 4.1. We show a guess for the result, the solid line in Fig. 4.1. This result means, that we expect no dramatic change of ΔE for the next Quarkonium. Only for quark masses well above 100 GeV the states would sit deeper and deeper in the V_{AF} singularity and ΔE starts to increase. Asymptotically the scaling behaviour of ΔE is $\alpha_s^2 m_Q \sim m_Q / \log^2(m_Q^2)$.

We now turn to level splittings and begin with the P waves. We have shown that the Fermi-Breit Hamiltonian (eq. 3.2) gives a reasonable description. From there we have

$$H^T, H_{AF}^{LS} \sim \frac{1}{m_Q^2} \left\langle \frac{1}{R} d_R\left(\frac{1}{R}\right) \right\rangle \sim \frac{1}{m_Q^2 R^3} \tag{4.7}$$

where H_{AF}^{LS} is the spin orbit term <u>without</u> the Thomas precession. In contrast the Thomas precession term behaves like

$$H_C^{LS} \sim \frac{1}{m_Q^2} \left\langle \frac{1}{R} d_R(R) \right\rangle \sim \frac{1}{m_Q^2 R} \tag{4.8}$$

The scaling behaviour of R (eq. 4.5) is somewhere between that in a log and in a linear potential, $R \sim m_Q^{-1/2} \ldots\ldots m_Q^{-1/3}$, and we can estimate the $^3P_2$ - $^3P_0$ splitting of more massive Quarkonium P waves shown in Table 4.1.

Quarkonium:	$c\bar{c}$(3.5 GeV)	$b\bar{b}$(9.8 GeV)	30 GeV
$M(^3P_2) - M(^3P_0)$ [MeV]	150 (input)	50-70	20-40

Table 4.1: P wave splittings in Quarkonia

A comparison of (4.8) with (4.7) shows one more important fact. The ratio of eq. (3.3) which is 0.5 in Charmonium should increase with m_Q and approach 0.8 asymptotically!

The spin spin splittings go essentially as $\alpha_s \cdot \Gamma_{e\bar{e}}$, which can be seen by combining eq. (3.9) with eq. (2.4). Experimentally $\Gamma_{e\bar{e}}$, normalized to the quark charge, is remarkably constant, Fig. 4.2. In the frame of nonrelativistic

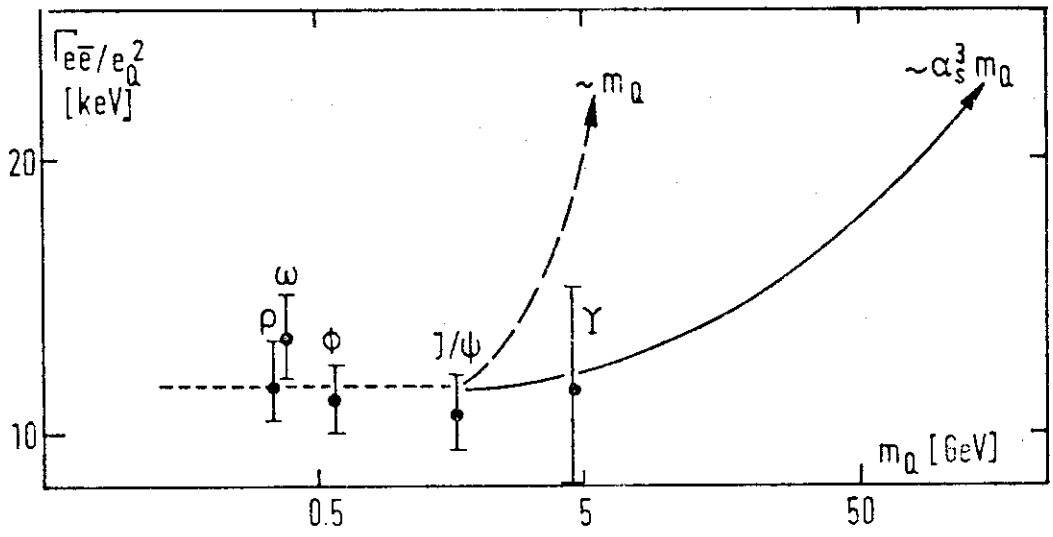

Fig. 4.2. Scaling behaviour of $\Gamma_{e\bar{e}}/e_Q^2$.
------- Experimental evidence below m_Q = 5 GeV
— — — in a pure Coulomb potential
——— in V_{AF} with $\alpha_s(M^2)$ via eq. (1.1)

potential models there is no way to explain this for ϱ, ω, ϕ . From J/ψ to Υ , however, we can use the scaling arguments. Table 4.2 shows the

Scaling in of	$V_{AF}(R) \sim -\frac{\alpha_s}{R}$	$V(R) \sim \log R$	$V_c(R) \sim R$
$\lvert\psi(0)\rvert^2 \sim R^{-3}$	$\alpha_s^3 \; m_Q^3$	$m_Q^{3/2}$	m_Q
$\Gamma_{e\bar{e}} \sim R^{-3} m_Q^{-2}$	$\alpha_s^3 \; m_Q$	$m_Q^{-1/2}$	m_Q^{-1}

Table 4.2: Scaling behaviour of $\lvert\psi(0)\rvert^2$ and $\Gamma_{e\bar{e}}$ in different potentials.

scaling behaviour of $\lvert\psi(0)\rvert^2$ and $\Gamma_{e\bar{e}}$ via eq. (2.4). $\lvert\psi(0)\rvert^2$ and therefore $\Gamma_{e\bar{e}}$ should feel more of the short distance potential than e.g. the level splittings. Numerical calculations indeed show almost m_Q-independence of $\Gamma_{e\bar{e}}$ in the range from Charmonium to Υ [28]. In the asymptotic limit $m_Q \longrightarrow \infty$, $\Gamma_{e\bar{e}} \sim \alpha_s^3 m_Q \sim m_Q \log^{-3}(m_Q^2)$, which also gives no net m_Q dependence from Charmonium to Υ . We are therefore led to plot this asymptotic m_Q dependence for $\Gamma_{e\bar{e}}$ starting with J/ψ.

This is done in Fig. 4.2 also.

The constancy of $\Gamma_{e\bar{e}}/e_Q^2$ below J/Ψ (Fig. 4.2), however, cannot be understood with our methods and we want to point out that it is a challenge to explain this fact together with the seemingly constancy of level spacings below 3 GeV, e.g., $M(A_2)-M(\rho) \simeq M(\chi 3.55) - M(J/\Psi)$.

The last aspect of scaling we discuss concerns the number of narrow $Q\bar{Q}$ states below the $Q\bar{q}\ \bar{Q}q$ threshold. The condition for a $Q\bar{Q}$ state to lie below the threshold for strong decays, can be written as

$$E_{Q\bar{Q}} < 2\, m_q + 2E_{Q\bar{q}} \tag{4.9}$$

with the binding energy $E_{Q\bar{q}} = M_{Q\bar{q}} - m_Q - m_{\bar{q}}$. The binding energy of $Q\bar{Q}$ states depends on the reduced mass of $Q\bar{Q}$ and therefore on the mass of the heavy quark Q. The states fall deeper in the potential well with increasing m_Q. The binding energy of $Q\bar{q}$, however, is in the first approximation independent of m_Q because the system is determined by the mass of the light quark q. This is of course an idealization, to be more sophisticated one would have to treat the relativistic binding problem of $Q\bar{q}$, or at least take into account the slight changes of the reduced mass $\mu = \frac{m_Q \cdot m_q}{m_Q + m_q}$ with m_Q and effects of the spin-spin interaction which depend stronger on m_Q (but are small). Taking $E_{Q\bar{q}}$ to be constant fixes the threshold for the binding energy $E_{Q\bar{Q}}$. The question one may pose then is: How many $Q\bar{Q}$ S wave states have a binding energy $E_{Q\bar{Q}}$ below this threshold? This question can be answered by semiclassical methods independent of the particular potential. The number n of bound S states below a given energy (r.h.s. of eq. (4.9) in this case) is given by the Bohr-Sommerfeld condition

$$\int_0^{R_0} dR\, \sqrt{m_q\,(E_{thr.} - V(R))} = \pi\,(n - 1/4) \tag{4.10}$$

where R_0 is the classical turning point, $V(R_0) = E_{thr.}$ [29]. For low numbers n (4.10) is only approximately valid (but maybe not worse than our other approximations) and we find

$$n \sim \text{const.} + \sqrt{\frac{m_q}{m_0}} \tag{4.11}$$

Quigg and Rosner fixed the constant of (4.11) in the Charmonium system ($m_Q = m_c$) and their result is displayed in Fig. 4.3. We can read off Fig. 4.3 that in the Υ system 3 S waves will be below the threshold

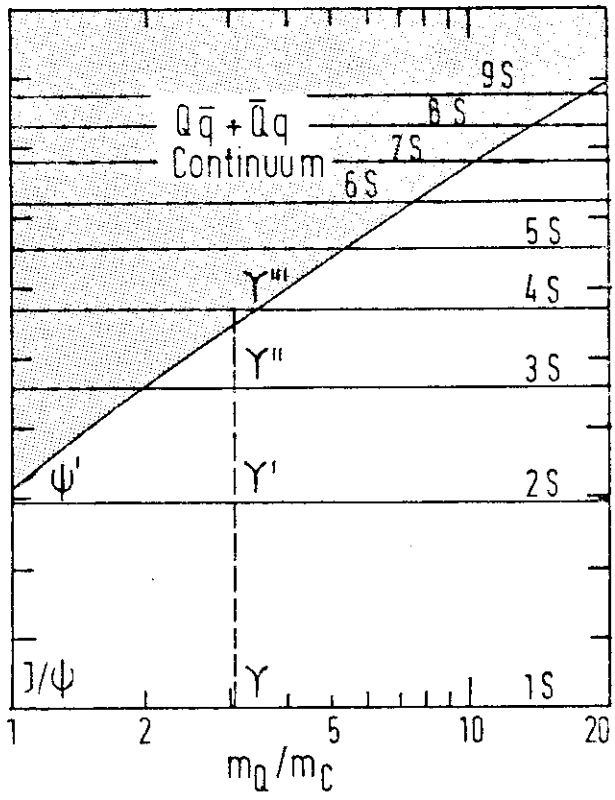

Fig. 4.3. Number of bound states below the strong decay threshold (Ref. 29). The Υ''' will be above the thresold.

of strong decays, the fourth, Υ''', may be even below $Q\bar{q}(\bar{Q}q)^*$ threshold. In any case Υ''' will decay into $B\bar{B}$ or $B\bar{B}^* \rightarrow B\bar{B}\gamma$, $B = Q\bar{q}$. The question for the actual threshold energy is not jet answered, to do that we would need calculations of the B masses, e.g. in a potential model. Unfortunately a potential model for the B mesons suffers from the relativistic motion of the light quark q inside the B. However, applying our knowledge about the number of bound Υ S waves, it is sufficient for us to know the masses of Υ'' and Υ''', since we already know the threshold relative to these. The latter masses are calculable much more reliably. In Table 4.3 the results of two orthogonal approaches are shown.

		Υ	Υ'	Υ''	Υ'''
Mass [a]	[GeV]	9.46 (input)	10.09	10.45	10.72
Mass [b]	[GeV]	9.46 (input)	10.02	10.34	10.60
$\Gamma_{e\bar{e}}$ [b]	[keV]	1.1	0.5	0.35	0.3

Table 4.3: Masses and $\Gamma_{e\bar{e}}$ of Υ radial excitations in the two orthogonal models of a) Ref. 30) and b) Ref. 20).

The model of Ref. 30) directly integrates the Bethe Salpeter equation for a $Q\bar{Q}$ system with a distant-dependent $\alpha_s(R)$. The second model, Ref. 20), is the phenomenologically successful modification of the standard model as discussed in Ch. 2. A look at Fig. and Table 4.3, and slightly rescaling the first model, convinces us that the $B\bar{B}$ threshold will be around 10.4 to 10.5 GeV.

Independently of the exact location of the threshold and the exact validity of Fig. 4.3 we expect that the first radial Υ excitation above the $B\bar{B}$ threshold is a "B-factory". (We think that this will be Υ''', of course). The reason is simply that in the decay of Υ''' to $B\bar{B}$ or $B\bar{B}^*$ the large number of radial nodes in the Υ''' wave function will suppress its decay width into two slowly moving ground state S waves like B or B^*. The width of Υ''' may therefore be well below the resonance machine width in e^+e^- production but, on the other hand, the branching fraction into $B\bar{B}$ (or $B\bar{B}^*$) should be substantial.

One comment on our saying "$B\bar{B}$ or $B\bar{B}^*$" is in order: Either the B-B^* splitting is as large (or larger) as the DD^* splitting, then B^* could decay in πB. But in this case Υ''' would lie below the $B\bar{B}^*$ threshold, as can be seen from Fig. 4.3. Or the B-B^* splitting is less than the D-D^* splitting (in non-relativistic potential models this splitting goes like $1/m_Q$ - but neither the D nor the B are nonrelativistic), then B^* decays to γB, which experimentally is almost as clean as a pure $B\bar{B}$ decay.

2nd LECTURE

The second lecture covers Quarkonium decays. We will first discuss the radiative photon transitions in E1 and M1 approximation and gluon transitions. These decays have in common that they depend on the medium and long distance behaviour of the wave function. We then (Ch. 6) turn to annihilations which are governed by the short distance behaviour of the wave functions. The annihilation can take place into photons and/or gluons. The gluons may form hadron jets. This is dealt with in Ch. 7.

5. Radiation

a) Electric Dipole Radiation

For photon or gluon wave lengths long against the bound state dimensions of Quarkonium one can try a multipole expansion. The widths of different multipole orders are typically [31]

$$\Gamma \sim \alpha e_Q^2 \left\{ \begin{matrix} k^3 R^2 \\ k^3 m_Q^{-2} \end{matrix} \right\} \cdot \left(\frac{kR}{2}\right)^{2(n-1)} \quad \text{for} \left\{ \begin{matrix} En \\ Mn \end{matrix} \right\} \text{transitions.} \tag{5.1}$$

up to numerical factors. k is the photon (gluon) wave number, R the bound state radius in the reduced system (R/2 is the true bound state radius). We see that the expansion parameter in (5.1) is $(k \cdot R/2)^2$ which is roughly 1/4 ... 3/100 in Charmonium and smaller in heavier Quarkonia. This justifies a multipole expansion and we will therefore confine ourselves to the lowest order transitions, E1 and M1.

In hydrogen the formula for an electric dipole transition (E1) is [31]

$$\Gamma^{E1}(|i\rangle \longrightarrow \gamma |f\rangle) = \frac{4}{3} \alpha k^3 |\vec{x}_{fi}|^2 \tag{5.2}$$

where $\vec{x}_{fi}$ is the matrix element of the dipole operator. In Quarkonia we now have three modifications to the case of eq. (5.2). First, <u>both</u> quarks can radiate, not only just one like the electron in hydrogen. Second, the

relevant mass is the reduced mass of the quark, $m_Q/2$, not just the particle mass like m_e in hydrogen. Third, the charge of the quark is only $e_Q \cdot e$. The first two modifications cancel each other, so that we are left with

$$\Gamma^{E1}(Q\bar{Q}_i \longrightarrow \gamma Q\bar{Q}_f) = \frac{4}{3} \alpha e_Q^2 \, k^3 \, |\vec{x}_{fi}|^2 \qquad (5.3)$$

in Quarkonium.

Of course, there are corrections to this naïve formula. The first one are higher multipoles. In ψ' decays they amount to at most 5 % if present (compare eq. (5.1)). The second one is an interference of the finite wave length of the photon field $e^{+ik\cdot R}$ with the bound state wave function. In atomic and nuclear transitions this interference is negligible, $\vec{k}\cdot\vec{R} \ll 1 \Longrightarrow e^{i\vec{k}\cdot\vec{R}} \simeq 1$. But in Quarkonium transitions higher terms of the expansion of $e^{i\vec{k}\cdot\vec{R}/2}$ will partly contribute to dipole transitions and tend to reduce the transition rate. However, Okun and Voloshin [32] have shown that this interference correction amounts to at most 5 % in Charmonium. The third but most important corrections are of relativistic nature. They consist of a) recoil corrections, b) relativistic corrections to the wave functions and c) the interaction of the quark magnetic moments with the electric vector of the photon field. The corrections of type c) have been studied by Okun and Voloshin [32]. They find correction factors between essentially 1.0 and 0.6.

The radiative widths of the standard model without corrections of the last type are given in Fig. 5.1 and Table 5.2. An example for the corrections of this type is shown in Table 5.1. The remaining discrepancy between theory

$\Gamma_{model}(\psi' \longrightarrow \gamma\, ^3P_j)$	$^3P_2$	$^3P_1$	$^3P_0$
without corr. [keV]	36	50	58
with corr. type c)	36	40	41

Table 5.1. Example for the magnitude of relativistic corrections to the naive dipole widths. [32]

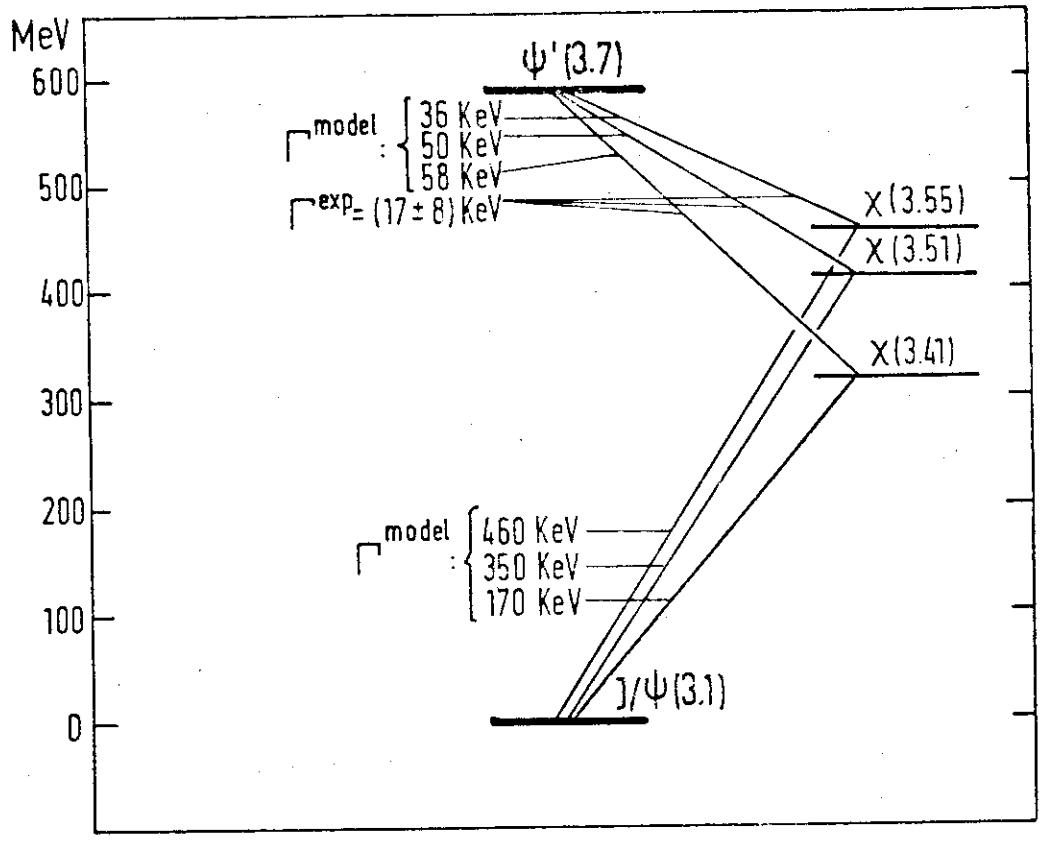

Fig. 5.1: E1 transitions in Charmonium. Model widths are calculated via eqs. (5.8) and (5.9) and do not include corrections.

(Table 5.1) and experiment (Fig. 5.1) might be due to relativistic corrections of type a) and b). The recoil corrections have been found to be $\approx$ + 20 % in a relativistic model [33]. In any case this indicates that also the model numbers for $\Gamma(\mathcal{P}_c/\chi \longrightarrow \gamma\, J/\psi)$ are only good within a factor 2.

b) E1 Sum Rules.

A very powerful tool for the discussion of electric dipole transitions has been rediscovered for Charmonium, namely the dipole sum rules [34]. We know two kinds of dipole sum rules, the so called Thomas-Reiche-Kuhn (TRK) sum rule and the Wigner (W) sum rule. Both apply to the dipole matrix element (eq. (5.3)) and any corrections like those discussed have to be done afterwards. The starting point for the dipole sum rules is Heisenberg's uncertainty relation

$$\left[\vec{x}, \vec{p}\right] = 3i \tag{5.4}$$

(we set $\hbar = c = 1$). In a static potential for $Q\bar{Q}$ without velocity dependent terms, e.g. no spin-orbit interaction, we can replace $\vec{p}$ via the equation of motion

$$\vec{p} = i \frac{m_Q}{2} \left[H^\circ, \vec{x}\right] \tag{5.5}$$

where H^0 is the Hamilton operator of the static potential, eq. (2.1). After taking the expectation value in a state $|i>$ and inserting a complete set of states $|f>$ this replacement of $\vec{p}$ leads to

$$\sum_f (E_f^\circ - E_i^\circ) \, |\vec{x}_{fi}|^2 = \frac{3}{m_Q} \tag{5.6}$$

Here E^0 are energy eigenvalues of H^0. The number of final states $|f>$ is restricted by selection rules. In an arbitrary static potential $\Delta\ell = \pm 1$ for dipole transitions. In a harmonic oscillator potential, however, the number of final states is further restricted by the oscillator selection rule: The change of the number of radial modes Δr is either 0 or $-\Delta\ell$. It follows that from the S wave ground state one can only reach the P wave ground state, from this 1 P wave one can reach the radially excited S wave, 2 S, the ground state, 1 S, and the D wave 1 D. These are all possible final states. We call this fact the saturation of the sum rule by the harmonic oscillator. To write down the first sum rules it is convenient to express the dipole operator $\vec{x}_{fi}$ through the radial operator R_{fi} [35]

$$\sum_{m'} |\langle r', \ell \pm 1, m' | \vec{x} | r, \ell, m \rangle|^2 = \left\{ \begin{matrix} \ell+1 \\ \ell \end{matrix} \right\} \frac{|\langle r', \ell \pm 1 | R | r, \ell \rangle|^2}{2\ell + 1} \tag{5.7}$$

where m is the magnetic quantum number. We can now write some rates (5.3) as

$$\Gamma(1P \longrightarrow \gamma\, 1S) = \frac{4}{9} \alpha e_Q^2 \, k^3 \, |R_{fi}|^2 \tag{5.8}$$

and

$$\Gamma\,(2^1S_0 \longrightarrow \gamma\, 1^1P_1) = \frac{4}{3}\,\alpha\, e_Q^2\, k^3\, |\,R_{fi}\,|^2 \tag{5.9a}$$

$$\Gamma\,(2^3S_1 \longrightarrow \gamma\, 1^3P_j) = \frac{4}{3}\,\frac{2j+1}{9}\,\alpha\, e_Q^2\, k^3\, |\,R_{fi}\,|^2 \tag{5.9b}$$

The TRK sum rule (5.6) gives us a bound

$$(E^\circ_{1P} - E^\circ_{1S})\,|\,R_{1P,1S}\,|^2 \leqslant \frac{3}{m_Q} \tag{5.10}$$

which implies an upper bound on $1P \longrightarrow 1S$

$$\Gamma(1P \longrightarrow \gamma 1S) \leqslant \frac{4}{9}\,\alpha\, e_Q^2 \cdot \frac{k^3}{k^{(0)}} \cdot \frac{3}{m_Q} \tag{5.11}$$

We can obtain more bounds with the help of the Wigner sum rule. Recall eq. (5.4). As an expectation value in state $|i\rangle$ it can be written as

$$\sum_f \langle i|\vec{x}|f\rangle\langle f|\vec{p}|i\rangle - \langle i|\vec{p}|f\rangle\langle f|\vec{x}|i\rangle = 3i \tag{5.12}$$

The angular selection rule now enables us to project out the final states with $\Delta\ell = +1$ and those with $\Delta\ell = -1$. We thus arrive at two sum rules after some elaborate algebra [35)]

$$\sum_{f,\ell-1} (E^\circ_f - E^\circ_i)\,|\,\vec{x}_{fi}\,|^2 = \frac{-\ell(2\ell-1)}{2\ell+1} \cdot \frac{1}{m_Q} \tag{5.13}$$

$$\sum_{f,\ell+1} (E^\circ_f - E^\circ_i)\,|\,\vec{x}_{fi}\,|^2 = \frac{(\ell+1)(2\ell+3)}{2\ell+1} \cdot \frac{1}{m_Q} \tag{5.14}$$

which of course add up to (5.6). We have gained two things: first, the number of final states on the l.h.s. of (5.13) and (5.14) is smaller than in the TRK sum rule, and second, (5.13) is negative, which is very helpful. For $\ell = 1$ in the initial state the first two terms of (5.13) give (using (5.7))

$$(E^0_{2S} - E^0_{1P})\,|R_{2S,1P}|^2 + (E^0_{1S} - E^0_{1P})\,|R_{1S,1P}|^2 \leq \frac{-1}{m_Q} \tag{5.15}$$

An upper bound for the second term on the l.h.s. is known from (5.10). This leaves us with

$$(E^0_{2S} - E^0_{1P})\,|R_{2S,1P}|^2 \leq \frac{2}{m_Q} \tag{5.16}$$

and we can deduce an upper bound on transition (5.9):

$$\Gamma(2^3S_1 \longrightarrow \gamma\, 1^3P_j) \leq \frac{4}{3}\,\frac{2j+1}{9}\,\alpha\, e_Q^2\,\frac{k^3}{k^{(0)}}\,\frac{2}{m_Q} \tag{5.17}$$

Next we will make use of the negative sign in eq. (5.13) with $\ell = 1$, the initial state being the $1P$ wave. The only contribution to (5.13) or (5.15) which is indeed negative is the transition to the 1S ground state. Its magnitude must be larger than the sum of all others! Therefore the knowledge of one of the other transitions, e.g. $2S \longrightarrow \gamma\, 1P$, gives us a lower limit on $1P \longrightarrow \gamma\, 1S$! We write (5.15) as

$$(E^0_{1P} - E^0_{1S})\,|R_{1S,1P}|^2 \geq \frac{1}{m_Q} + (E^0_{2S} - E^0_{1P})\,|R_{2S,1P}|^2 \tag{5.18}$$

and obtain by "inverting" (5.17)

$$\Gamma(1^3P_j \longrightarrow \gamma\, 1^3S_1) \geq \frac{4}{9}\alpha e_Q^2\,\frac{k^3}{k^{(0)}}\,\frac{1}{m_Q} + \frac{3}{2j+1}\,\frac{k^3_{1P,1S}}{k^3_{2S,1P}}\,\frac{k^{(0)}_{2S,1P}}{k^{(0)}_{1P,1S}}\,\Gamma^{exp}(2^3S_1 \to \gamma\, 1^3P_j) \tag{5.19}$$

The W sum rule gave us an upper bound on $2S \longrightarrow \gamma\, 1P$ and a lower bound on $1P \longrightarrow \gamma\, 1S$. The TRK sum rule gave us an upper limit on the latter transition. We combine all our information in Table 5.2. Combining the bounds of Table 5.2 and the experimentally

transition	TRK SR	W SR	model
$2^3S_1 \longrightarrow \gamma\, 1^3P_2$		< 40	36
$2^3S_1 \longrightarrow \gamma\, 1^3P_1$		< 56	50
$2^3S_1 \longrightarrow \gamma\, 1^3P_0$		< 64	58
$1^3P_2 \longrightarrow \gamma\, 1^3S_1$	< 490	> 160 + 140	460
$1^3P_1 \longrightarrow \gamma\, 1^3S_1$	< 370	> 125 + 75	350
$1^3P_0 \longrightarrow \gamma\, 1^3S_1$	< 180	> 60 + 30	170

Table 5.2: Upper and lower limits on E1 transitions from the Thomas-Reiche-Kuhn (TRK) and Wigner (W) sum rules (SR). All widths in keV. The second numbers in the lower half of the W SR column arise from the second term r.h.s. of (5.19). The quark mass is taken to be m_c = 1.6 GeV.

measured BRs for $P_c/\chi \longrightarrow \gamma\, J/\psi$ one can deduce bounds for the total widths of the P states in Charmonium. This is shown in Table 5.3.

P states	$\chi(3.41) = 0^{++}$	$P_c/\chi(3.51) = 1^{++}$	$\chi(3.55) = 2^{++}$
BR($\gamma J/\psi$), exp. [%]	3 ± 3	35 ± 7	14 ± 6
$\Gamma_{tot}(P_c/\chi)$, bounds [MeV]	3 ... 6	0.57...1.05	2.15...3.5

Table 5.3: Bounds on $\Gamma_{tot}(P_c/\chi)$ derived from the sum rules, Table 5.2, and the experimental BRs of $P_c/\chi \longrightarrow \gamma\, J/\psi$. The sum rules correspond to an uncorrected E1 transition, this gives an additional theoretical uncertainty of a factor 2.

The total widths of the P_c/χ states should be calculable as the sum of the radiative widths plus the gluon annihilation widths. A comparison of these total widths with the bounds of Table 5.3 will be a comparison of theory with "experiment". We will do that in a forthcoming chapter.

c) Magnetic Dipole Transitions.

M1 decays arise from an interaction of the magnetic photon field vector $\vec{m} = \vec{k} \times \vec{\varepsilon}$ and the quark magnetic moment $\mu_Q = e \cdot e_Q / 2 m_Q$. The matrix element therefore reads

$$\langle f | \mu_Q \vec{\sigma} \cdot (\vec{k} \times \vec{\varepsilon}) | i \rangle \tag{5.20}$$

and acts on the spin part of the states $|i\rangle$ and $|f\rangle$ only. Again we have two graphs for the emission of a photon and therefore 4 times the rate as in atomic M1 transitions [31]

$$\Gamma(V \longrightarrow \gamma PS) = \frac{16}{3} \mu_Q^2 k^3 \delta^{rr'} = \frac{4}{3} \alpha e_Q^2 \frac{k^3}{m_Q^2} \delta^{rr'} \tag{5.21}$$

$$\Gamma(PS \longrightarrow \gamma V) = 3 \Gamma(V \longrightarrow \gamma PS)$$

An M1 transition requires $\Delta \ell = 0$ and the spatial overlap between the two states $|i\rangle$ and $|f\rangle$ with number of radial nodes r and r' is either $1(r = r')$ or $0(r \neq r'$, forbidden M1) in this approximation. Relativistic corrections of course modify the rate (5.21) and lead to small transitions also between orthogonal $(r \neq r')$ states. In allowed M1 transitions $(r = r')$ the spatial overlap of 1 cannot be changed much by relativistic corrections.

d) Scaling of E1 and M1.

Before we now discuss the M1 transitions in charmonium, let us look at the scaling behaviour of both kinds of dipole transitions. For E1 transitions the scaling behaviour is most easily obtained from the sum rules.

$$\Gamma \sim \frac{k^3}{k^{(0)}} \frac{1}{m_Q} \approx \frac{k^2}{m_Q} \tag{5.22}$$

M1 transitions, on the other hand, scale like

$$\Gamma \sim \mu_Q^2 k^3 \sim \frac{k^3}{m_Q^2} \qquad (5.23)$$

i.e. $\Gamma(M1) \sim \Gamma(E1) \cdot k / m_Q$. Since in the next heavy Quarkonia k does not increase with m_Q the relative magnitude of M1 compared to E1 goes down at least like $1/m_Q$. A comparison of related radiative transitions in different Quarkonia can thus help to distinguish E1 from M1 transitions!

e) Problems with M1 in Charmonium.

In Fig. 5.2 possible candidates for the pseudoscalars and the corresponding M1 transitions are shown. If the second χ is not at 3.59 GeV but at 3.18 GeV (second experimental solution) it can hardly be explained as a pseudoscalar. In Fig. 5.2 the calculated M1 widths are shown. They have

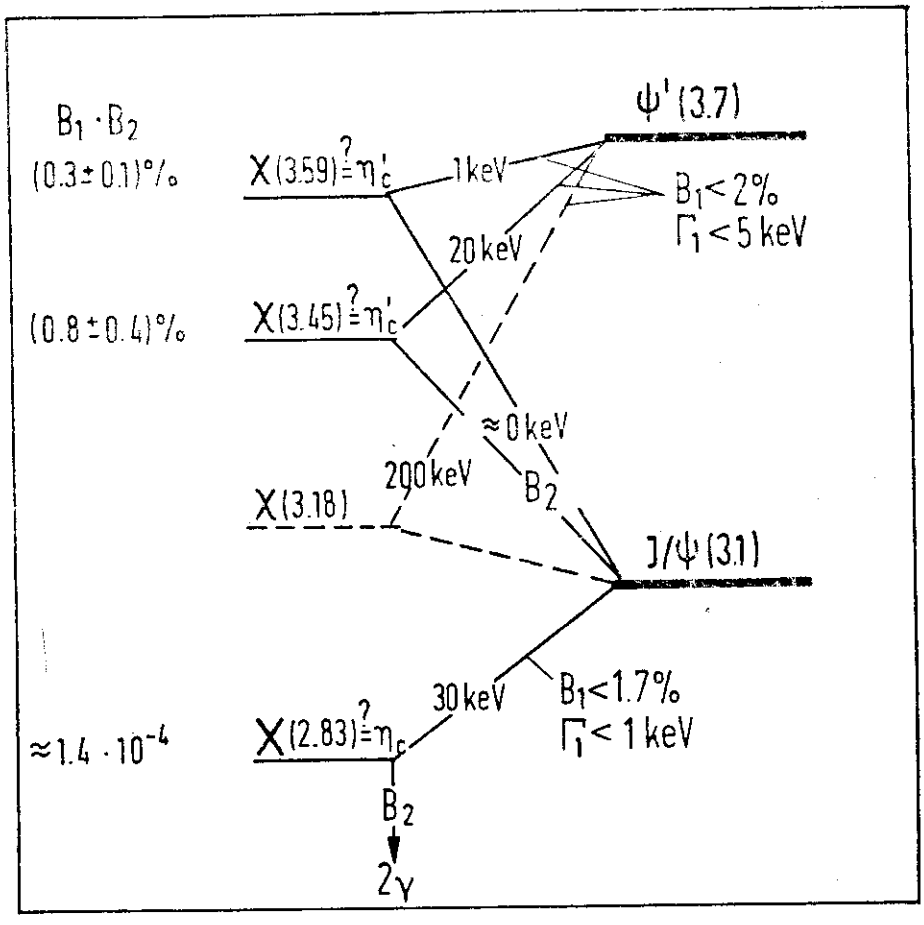

Fig. 5.2: M1 transitions in Charmonium. Theoretical widths, eq. (5.21) are indicated at the transition lines. $B_1(\Gamma_1)$ and $B_1 \cdot B_2$ are from experiment, Ref. 1)+ 36).

at first to be contrasted with the experimental bound on these transitions as indicated. Together with the experimental product of branching ratios these bounds allow to derive lower limits on the decay branching fractions of these states. This is shown in Table 5.4. There is no way of assigning

State	$\chi(3.59)$	$\chi(3.45)$	$\chi(2.83)$
$B_1 \cdot B_2$ (Exp.) [%]	0.3 ± 0.1	0.8 ± 0.4	0.014 ± 0.004
B_1 (Exp.) [%]	< 2	< 2	< 1.7
B_1 (Theory) [%]	$\simeq 0.5$	$\simeq 9$	$\simeq 45$
B_2 (Exp.) [%]	> 10	> 20	> 0.7
B_2 (Theory) [%]	< 1	< 1	≈ 0.1

Table 5.4: Experimental upper bounds on B_1 and lower bounds on B_2 via $B_1 \cdot B_2$, and comparison with theory. The kind of transition for B_1, B_2 is indicated in Fig. 5.2. The theoretical numbers arise from allowed and "forbidden" M1 transitions and the ratio of 2γ versus 2 gluon annihilation. For the latter see Chapter 6. The forbidden M1 transition should lead to a B_2 not bigger than a few 10 keV/a few MeV $\approx 10^{-2}$.

one of the experimental states to a pseudoscalar state without coming in trouble with a) absolute M1 widths, b) branching fractions for the decay of this state. Considering η_c and η_c' in context leads to even larger discrepancies, e.g. take $\chi(3.59)$ as η_c' and $\chi(2.83)$ as η_c. Then the M1 transition $J/\psi \longrightarrow \gamma \eta_c$ is down by a factor of 30 compared to the naive theory. The same factor must work in $\psi' \longrightarrow \gamma \eta_c'$ leading to $\Gamma_1 = 1/30$ keV and consequently to $B_2 > 30$! For M1 widths only one unpleasant way out seems possible: to give the quarks a vanishing magnetic moment μ_q in this limit of a static interaction [37].

A much more pleasant way out would be finding the true pseudoscalars much nearer to J/ψ and ψ' respectively. Experimentally this is in no way ruled out. Then the χ and χ states are either not real or at least no simple

$Q\bar{Q}$ states [38]. Remember that QCD is consistent with a possible existence of multiquark or multiquark-gluon states different from $Q\bar{Q}$ [39]. However, their properties are not accessible in our simple Quarkonium model.

f) Gluon Radiation

Radiative gluon transitions can be subject to a similar multipole expansion as electromagnetic radiation. While the expansion in $(k \cdot R/2)^2$ might converge, the expansion in α_s/π needs not. The distances involved in the process are of the order of the wave function radius and α_s will be large. This is the essential reason why we do not expect to be able to calculate rates for gluon radiation. But we might be able to estimate the scaling behaviour of such radiation. The processes which are described as gluon radiation in QCD are typically

$$2^3S_1 \longrightarrow 1^3S_1 + n\,g \qquad (5.24)$$
$$\hookrightarrow \varepsilon, \eta, \ldots$$

The emitted states must be Isosinglets, because gluons carry no Isospin. For the radiation of an ε ($\pi\pi$ S wave) from 2^3S_1 Gottfried [40] estimates an $1/m_Q^2$ behaviour of the matrix element

$$\Gamma(2^3S_1 \longrightarrow 1^3S_1 + \varepsilon) \sim \frac{1}{m_Q^2} \cdot \text{Phase space} \qquad (5.25)$$

If this scaling law is already valid in the Charmonium system, $\psi' \longrightarrow \pi\pi\ J/\psi \approx 100$ keV implies $\Upsilon' \longrightarrow \pi\pi\ \Upsilon \simeq 10$ keV. In a 30 GeV $Q\bar{Q}$ system this width would be no more than 1 keV. Transitions via gluon radiation will be important for a search for $Q\bar{Q}$ states which are not accessible directly or via photon transitions, like the 1^1P_1 state. In the Υ or higher $Q\bar{Q}$ systems the 3^3S_1 state (Υ'' e.g.) will be narrow and undergo such a transition to the 1^1P_1 state.

$$3^3S_{1--} \longrightarrow 1^1P_{1+-} + \eta, \varepsilon \qquad (5.26)$$

The finding of a 1^1P_1 state via (5.26) would be very interesting because the knowledge of the 1^1P_1 mass allows to determine, whether there are long

range spin spin correlations or not. In our Ansatz for the Hamiltonian and potential we only had short range spin spin forces. They do not act on P waves and therefore the 1^1P_1 state is degenerate with the c.o.g. of the 1^3P states. A long range spin spin force, however, would act on the P waves and would lift this degeneracy.

6. Annihilation

Quarkonium states may annihilate into photons and/or gluons. Since annihilation is a pointlike process (the quarks must come together) not only the annihilation into photons is governed by a small coupling $\alpha = 1/137$, but hopefully also that into gluons by α_s(small R) . We can apply the 'minimal gluon scheme', i.e. approximate the decay by the lowest order (Born-) graph [41]. This will be justified by finding that indeed the α_s(annihilation) is small, even in Charmonium it is much smaller than the effective α_s for the bound state description (see Chapter 2). We proceed in the following way. First we collect well known formulae for annihilations in Born approximation. In this approximation there is no gluon selfinteraction yet, so that the conversion from photon annihilations to gluon annihilations is just done by redefining the charge. We will then discuss ratios of these widths as an application in Quarkonia. Our results will also be fundamental for the next chapter on jets.

a) Annihilation Formulae.

The vector $^3S_1$ ground state can decay via one photon into lepton or quark pairs (hadrons). The corresponding graph is displayed in Fig. 6.1 and the formula is known as V.Royen-Weisskopf formula[42] (including colour and for $4m_e^2 \ll M_V^2$):

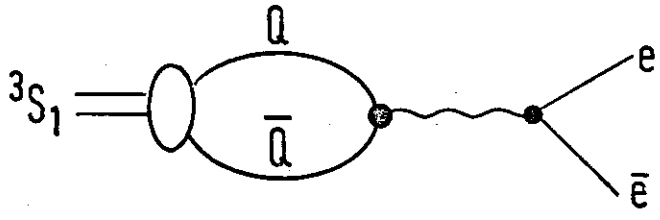

Fig. 6.1: Leptonic decay of $^3S_1(Q\bar{Q})$. The electrons may be replaced by μs, τs or quarks lighter than Q.

$$\Gamma_{e\bar{e}}(V) = 16\pi\alpha^2 e_Q^2 \frac{|\Psi(0)|^2}{M_V^2} \simeq \alpha^2 e_Q^2 \frac{|R(0)|^2}{m_Q^2} \qquad (6.1)$$

where M_V is the $V = {}^3S_1$ bound state mass and $m_Q \simeq 1/2\ M_V$ the quark mass. $\Psi(o)$ is the spatial and $\mathcal{R}(o)$ the radial wave function at the origin. Quarks couple in the same way to the photon as leptons, so that (6.1) is understood for each lepton or quark flavour separately: $\Gamma_{q\bar{q}} = 3e_q^2\,\Gamma_{e\bar{e}}$.

The decay of ${}^3S_1$ into two photons as well as two gluons is impossible. In the two photon case this is just the photon C parity. Also two gluons, as long as they are in a colour singlet state (which is symmetric), have even C. But the ${}^3S_1$ can decay into three photons as well as three gluons, Fig. 6.2. The three photon decay has been calculated by Ore and Powell [43] (here including the statistical colour factor)

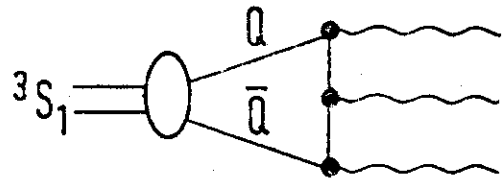

Fig. 6.2: 3γ decay of ${}^3S_1(Q\bar{Q})$. When the photons are replaced by gluons, this denotes the "direct" hadronic decay.

$$\Gamma_{3\gamma}(V) = \frac{4}{3}\,\alpha^3 e_Q^6\,\frac{\pi^2 - 9}{\pi}\,\frac{|\mathcal{R}(0)|^2}{m_Q} \tag{6.2}$$

The conversion factor to the three gluon decay is [44]

$$\Gamma_{3g}/\Gamma_{3\gamma} = \frac{\alpha_s^3}{\alpha^3 e_Q^6}\,\frac{1}{9}\sum{}'_{a,b,c}\left[\mathrm{Tr}\left(\frac{\lambda^a}{2}\,\frac{\lambda^b}{2}\,\frac{\lambda^c}{2}\right)_{sym.}\right]^2 \tag{6.3}$$

so that we have

$$\Gamma_{3g}(V) = \frac{10}{81}\,\alpha_s^3\,\frac{\pi^2 - 9}{\pi}\,\frac{|\mathcal{R}(0)|^2}{m_Q{}^2} \tag{6.4}$$

The parts of (6.3) have the following origin. $\alpha_s^3/\alpha^3 e_Q^6$ just converts the charges together with $\mathrm{Tr}\,(\lambda^a/2\ \lambda^b/2\ \lambda^c/2)_{sym.}$. The Σ_{abc} counts the number of coloured graphs in the 3g case, while the 3^{-2} counts the number of coloured graphs in the 3γ case. We do not consider decays of the ${}^3S_1$ into more ($\geqslant 5$) photons or ($\geqslant 4$) gluons.

The pseudoscalar ${}^1S_0$ ground state can decay into two photons or two gluons, Fig. 6.3. The two photon decay was first calculated by Pomeranchuk [45] and

is (including colour)

$$\Gamma_{2\gamma}(PS) = 3\alpha^2 e_Q^4 \frac{|R(0)|^2}{m_Q^2} \tag{6.5}$$

With the conversion factor

$$\Gamma_{2g}/\Gamma_{2\gamma} = \frac{\alpha_s^2}{\alpha^2 e_Q^4} \frac{1}{9} \sum_{a,b} \left[Tr\left(\frac{\lambda^a}{2} \frac{\lambda^b}{2}\right) \right]^2 \tag{6.6}$$

whose components are described in the case of eq.(6.3) one obtains

$$\Gamma_{2g}(PS) = \frac{2}{3} \alpha_s^2 \frac{|R(0)|^2}{m_Q^2} \tag{6.7}$$

We do not discuss the decay of $^1S_0$ in more ($\geq$4) photons or ($\geq$3) gluons. Assuming, that the 2g decay is the basic process for the dominant hadronic decay of the pseudoscalar, allows to derive the branching fraction for the 2γ-decay (Table 5.4) from eq.(6.6).

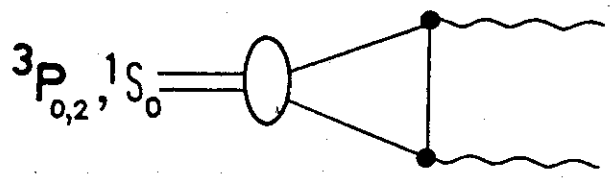

Fig. 6.3: 2γ-decay of $Q\bar{Q}$. For the hadronic decay the photons are replaced by gluons.

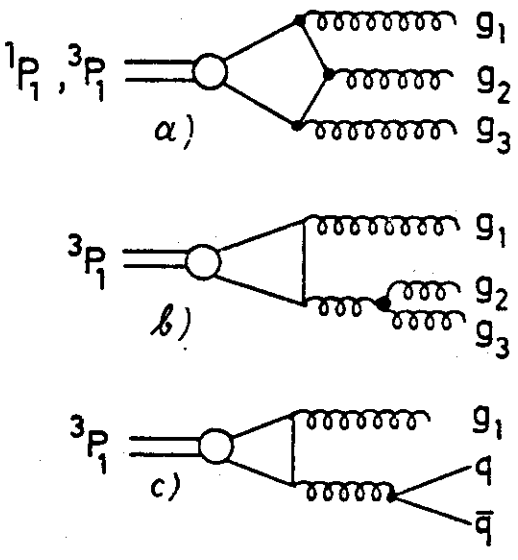

Fig. 6.4: The gluonic decay diagrams of spin 1 P waves.

We now turn to P wave annihilation, Fig.6.3 and 6.4. Here life is more complicated because the wave function of a P wave at the origin is zero. That means that the quarks do not like to come together to annihilate: The annihilation widths of P waves will be smaller than that of the $^1S_0$ wave! The P waves, however, can annihilate when the two quarks come near each other and simultaneously have a relative velocity $\neq 0$. This is a higher order process in terms of an expansion in $\beta^2=(v/c)^2$. It is governed by the spatial derivative of the wave function. In this approximation the widths of the spin 0 and spin 2 P waves of Positronium

have first been calculated by Alekseev [46]. The same calculation for Charmonium has been done by Barbieri, Gatto and Kögerler [47]. They yield

$$\Gamma_{2g}(^3P_0) = 6\alpha_s^2 \frac{|R'(0)|^2}{m_Q^4} \tag{6.8}$$

$$\Gamma_{2g}(^3P_2) = \frac{8}{5}\alpha_s^2 \frac{|R'(0)|^2}{m_Q^4} \tag{6.9}$$

The 2γ widths of $^3P_{0,2}$ can be obtained from (6.8) and (6.9) by the conversion factor given in eq. (6.6).

The decays of the j = 1 P waves are more complicated. A spin 1 state cannot decay into two massless vector bosons, either photons or gluons in a colour singlet [48]. We therefore have to consider the next order (in α_s) diagrams, which for gluon annihilation are shown in Fig. 6.4. They bring up another complication. We now have a three body phase space and have to integrate over all possible energies of, say, gluon 1. Gluon 1 is allowed to be soft. It further is allowed to carry away the angular momentum of the P wave. So it has all characteristics of a bremsstrahlungs gluon. The same is true for photon annihilation, except that in this case diagram b) of Fig. 6.4 is absent. A bremsstrahlungs gluon or photon in the annihilation of a free $Q\bar{Q}$ pair with $\ell = 1$ leads to the typical bremsstrahlungs singularity. The cross section factorizes into the bremsstrahlungs part and the annihilation of an $\ell = 0$ $Q\bar{Q}$ pair into two photons or gluons. For a bound state, however, the annihilation amplitude cannot be singular, because the quarks are not on shell. Their virtuality is of the order of the bound state dimensions. For a bound state annihilation we therefore may cut the amplitude at momenta of the soft (bremsstrahlungs) photon or gluon which correspond to the bound state radius. In diagram language, the singularity will be cancelled by higher order graphs like vertex corrections. For QED this procedure is well defined [49]. We hope that it will work parallel for QCD. As a cutoff momentum for QCD annihilation we take the typical momentum for a soft "confinement" gluon, 400 MeV, since in a QCD process higher order graphs will involve such "confinement" gluons. We will express the cutoff in terms of a parameter $\Delta = 2M \cdot 400$ MeV [50], M being the Quarkonium

bound state mass. Let us first discuss the $^1P_1$ decay. This state has $j^{PC} = 1^{+-}$ and therefore only diagram a) of Fig. 6.4 can contribute, in either photon or gluon annihilation. Its decay has been calculated by Barbieri, Gatto and Remiddi [49]. They find

$$\Gamma_{3g}\,(\,^1P_{1^{+-}}) \simeq \frac{20}{9}\,\alpha_s^3\,\frac{|R'(0)|^2}{m_Q{}^4}\,\log\frac{M^2}{\Delta} \qquad (6.10)$$

where the log arises from the bremsstrahlungs singularity of the diagram. For the decay of the $^3P_1$ state, $j^{PC} = 1^{++}$, only diagram c) can contribute to the photon annihilation while in principle all three diagrams can contribute to the gluon annihilation. Barbieri, Gatto and Remiddi [49] found that the singular parts of the diagrams a) and b) cancel each other. Okun and Voloshin [32] gave the general argument for this: The amplitudes a) and b) interfere, since they lead to the same final state. Since they can both be factorized into the bremsstrahlungs part times the corresponding annihilation diagram for the 2 gluon annihilation of a coloured $^3S_1$ state, also their sum can be factorized in this way. This sum, however, contains all graphs to this order for $^3S_1$ (coloured) $\longrightarrow$ 2g, which must be zero [32]. Neglecting the non-singular parts of amplitudes a) and b) against the singular c) means that also for the gluon annihilation the calculation of graph c) is sufficient. It gives [49,50]

$$\Gamma_{gq\bar{q}}\,(\,^3P_{1^{++}}) \simeq \frac{N}{3}\,\frac{8\,\alpha_s^3}{3\pi}\,\frac{|R'(0)|^2}{m_Q{}^4}\left(\log\frac{M^2}{\Delta} - \frac{1}{2}\right) \qquad (6.11)$$

where N is the number of light flavours q. The photon versions of (6.10) and (6.11) can be found in Ref. 32).

For completeness we note the formula for the decay of the spin 2 D wave into 2 gluons which is given by the second derivative of the wave function, this is the second order in an expansion of $\beta^2 = (v/c)^2$ and therefore even less reliable. Okun and Voloshin [32] calculated

$$\Gamma_{2g}\left({}^1D_2\right) = \frac{2}{3}\,\alpha_s^{\,2}\,\frac{|R''(0)|^2}{m_Q^{\,6}} \tag{6.12}$$

b) Ratios and Applications.

The ratio of eqs. (6.4) and (6.1) gives

$$\frac{\Gamma({}^3S_1 \longrightarrow 3g)}{\Gamma({}^3S_1 \longrightarrow e\bar{e})} = \frac{10}{81}\cdot\frac{\pi^2-9}{\pi}\cdot\frac{\alpha_s^{\,3}}{\alpha^2 e_Q^{\,2}} \simeq 1440\,\frac{4}{9e_Q^{\,2}}\,\alpha_s^{\,3} \tag{6.13}$$

If we interpret as usual the 3g annihilation as the total direct hadronic annihilation then this is a measurable quantity and we have e.g. in Charmonium

$$\frac{\Gamma(J/\psi \longrightarrow hadr)_{dir.}}{\Gamma(J/\psi \longrightarrow e\bar{e})} \simeq 10 \tag{6.14}$$

from which follows that the α_s at <u>annihilation distances</u> is $\alpha_s \simeq 0.19$. Because of the third power of α_s in (6.13) this value is quite stable even against large corrections on the widths. The kinds of corrections we have discussed to eq. (6.1) at the end of Ch. 3 and different ones for Γ_{3g} will not be able to achieve an agreement between α_s(spectrum) $\simeq 0.4$ and α_s(annihilation) $\simeq 0.2$ in the Charmonium system. But this discrepancy does not surprise, as we have discussed in Chapter 1.

A very interesting ratio is that of eq. (6.8) to eq. (6.10) to eq. (6.9):

$$\Gamma_{2g}({}^3P_{0^{++}}) \;:\; \Gamma_{gq\bar{q}}({}^3P_{1^{++}}) \;:\; \Gamma_{2g}({}^3P_{2^{++}}) \tag{6.15}$$

$$= \quad 15 \quad : \quad \frac{20\,N\,\alpha_s}{9\pi}\left(\log\frac{M^2}{\Delta}-\frac{1}{2}\right) : \quad 4$$

It leads to ratios of

$$15 : 2.1\alpha_s : 4 \qquad J/\psi$$
$$15 : 5.7\alpha_s : 4 \quad \text{in the} \quad \Upsilon \quad \text{system.} \qquad (6.16)$$
$$15 : 11\alpha_s : 4 \qquad 30\ \text{GeV}\ Q\bar{Q}$$

We can of course calculate more than these ratios, namely the total widths of the P waves, assuming that these are given by the gluon annihilation width and radiative transition width essentially. The result is shown in Table 6.1

		$\Gamma_{tot}(^3P_0)$ [MeV]	$\Gamma_{tot}(^3P_1)$ [MeV]	$\Gamma_{tot}(^3P_2)$ [MeV]
$c\bar{c}$	theory	4	0.5	1.5
	"quasiexp."	6 ± 6	1 ± 0.2	3.2 ± 1.6
$b\bar{b}$	$\alpha_s = 0.15$	0.35	0.05	0.15
	$\alpha_s = 0.2$	0.6	0.08	0.2

Table 6.1: Comparison of "experiment" and theory for the P wave total widths, including the radiative transitions. The "experiment" line is taken from Tables 5.2 and 5.3. The prospects of the Υ system are also given.

for charmonium and the Υ system, and compared to the quasiexperimental bounds of Table 5.3. For the calculation of eqs. (6.8) ... (6.10) we need $|R'(0)|^2$. Numerical calculations give $|R'_{c\bar{c}}(0)|^2 m_c^{-4} \simeq 15\ MeV$ and $|R'_{b\bar{b}}(0)|^2 m_b^{-4} \simeq 2.5$ MeV. These quantities are relatively quark mass independent. We conclude that although the widths of Table 6.1 are very model dependent, the pattern of (6.16) agrees very well with the observed branching ratios of the Charmonium P waves. This is one of the successful predictions of QCD within Charmonium.

We complete our discussion of ratios of widths with a discussion of the $^3S_1$ decays. The decay channels of the vector ground state are: i) into lepton pairs, $e\bar{e}$, $\mu\bar{\mu}$, $\tau\bar{\tau}$, ii) into hadrons, $\sum q\bar{q}$, the ratio of ii) against

i) is essentially given by the famous R, iii) the three gluon annihilation, and iv) the annihilation into one photon and two gluons. The only ratio missing so far is that of iv) to iii). We can estimate it by comparing the electromagnetic and strong coupling for one fermion-boson vertex and by taking into account the different coupling of the colours of two versus three gluons

$$\frac{\Gamma(^3S_1 \longrightarrow \gamma gg)}{\Gamma(^3S_1 \longrightarrow 3g)} = \frac{36}{5}\,\frac{\alpha e_Q^2}{\alpha_S} \qquad (6.17)$$

$c\bar{c}$ decay channel:	$e\bar{e}+\mu\bar{\mu}$: $\sum q\bar{q}$: 3g : γ 2g			
$e_Q = 2/3$	2 : R : $\frac{5}{18}\frac{\pi^2-9}{\pi}\frac{\alpha_S^3}{\alpha^2}$: $\frac{8}{9}\frac{\pi^2-9}{\pi}\frac{\alpha_S^2}{\alpha}$			
a) $\alpha_S = 0.19$	2 : 2.5 : 10 : 1.2			
$b\bar{b}$ decay channel:	$e\bar{e}+\mu\bar{\mu}$: $\sum q\bar{q} + \tau\bar{\tau}$: 3g : γ 2g			
$e_Q = -1/3$	2 : R : $\frac{20}{18}\frac{\pi^2-9}{\pi}\frac{\alpha_S^3}{\alpha^2}$: $\frac{8}{9}\frac{\pi^2-9}{\pi}\frac{\alpha_S^2}{\alpha}$			
b) $\alpha_S = 0.15$	2 : 5 : 20 : 0.8			
$\alpha_S = 0.18$	2 : 5 : 34 : 1.1			
$t\bar{t}$ (30 GeV) decay channel :	$e\bar{e}+\mu\bar{\mu}$: $\sum q\bar{q}+\tau\bar{\tau}$: 3g : γ 2g			
$e_Q = 2/3$	2 : R : $\frac{5}{18}\frac{\pi^2-9}{\pi}\frac{\alpha_S^3}{\alpha^2}$: $\frac{8}{9}\frac{\pi^2-9}{\pi}\frac{\alpha_S^2}{\alpha}$			
c) $\alpha_S = 0.12$	2 : 5 : 2.5 : 0.5			
$\alpha_S = 0.15$	2 : 5 : 5 : 0.8			

Table 6.2: Ratios of the ground state decay channels a) in Charmonium, b) in the Υ system, c) in a 30 GeV $t\bar{t}$ system. For Charmonium $\alpha_S = 0.19$ agrees with experiment (lowest order formulae). For Υ decays the value of α_S best compatible with experiment, $B_{\mu\bar{\mu}}$ [52], seems to be 0.18 at present.

For Charmonium three exclusive contributions to $^3S_1 \to \gamma gg$ have been seen so far. namely $J/\psi \longrightarrow \gamma\eta\,,\ \gamma\eta'\,,\ \gamma f$ [51]. Together with eq. (6.13) this is all we need to put up Table 6.2.

7. Jets

The exploration of QCD suffers from the fact that its constituents, the quarks and gluons,cannot exist as free particles because of the confinement. Their properties cannot be investigated directly. But there is a surrogate for the observation of the free constituents, that are the jets. Experimentally jets are observed not only in deep inelastic hadron-hadron and lepton-hadron scattering but especially in e^+e^- annihilation, once the c.m. energy of 5 GeV is exceeded. The angular distribution of these jets is completely consistent with the production of two spin 1/2 (almost) massless particles [53], the quarks, via photon vacuum polarisation. The fragmentation of quarks into hadrons is imagined as a nonperturbative confinement effect, which conserves the original directed momenta.

At present there is no way of calculating this process, but there exists a very suggestive picture: Inside a small space region of ≈1/2 fm colour can exist and within this region the $q\bar{q}$ pair (or gluon) production is a short distance effect (see Fig. 7.1). When hard coloured quanta (quarks or gluons) with momenta p_i reach the confinement sphere they must fragment into white hadrons since colour fields cannot exist outside this sphere. The coloured quanta break up into hadrons with a finite perpendicular momentum $\vec{p}_\perp$. This breaking up is energetically much favoured over a further existence as coloured quanta. When the perpendicular momenta are small compared to the longitudinal hadron momenta, which add up to the momentum of the original quantum, we see hadron jets. The confinement effects, however, are assumed to be soft, carried by long wavelength quarks and/or gluons. The wavelength corresponds to the colour bag of 1/2 fm. Therefore the jet momenta equal the original quantum momenta up to

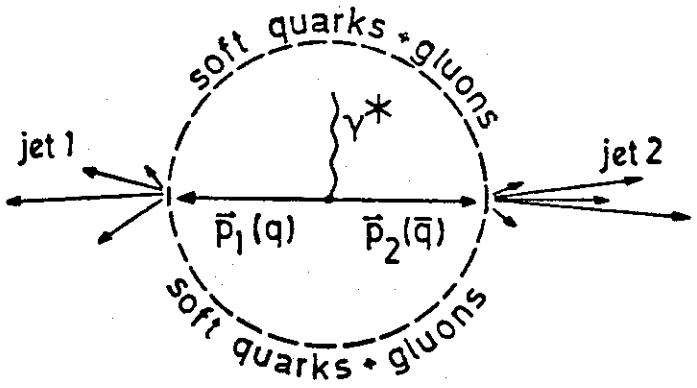

Fig. 7.1. Quark jets.

the order of 400 MeV. This picture demands the production of the original jet quanta to be a short distance effect ($\ll 1/2$ fm). This is certainly true for the (electromagnetic) quark pair production in e^+e^-. It is also true for a hard gluon bremsstrahlung process [54]. Resonance decays, however, are not pointlike but involve propagators (Fig. 7.2 and 6.2). Here it is not so clear, how well the jet picture will work. However, because the propagators are mass dependent the picture will work the better the higher the mass of the decaying $Q\bar{Q}$ resonance is. For a Q-mass of 5 GeV the propagator length in Fig. 7.2 is probably already short enough to apply the jet picture and for the next new flavour (higher) $Q\bar{Q}$ resonance it will definitely be so.

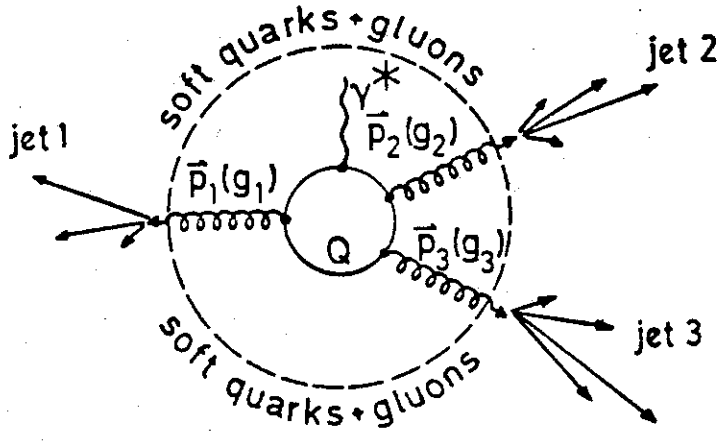

Fig. 7.2. $Q\bar{Q} \longrightarrow$ 3 gluon jets.

The quark jets in e^+e^- annihilation became visible above $s = (p_1+p_2)^2 \gtrsim (5\ \text{GeV})^2$, i.e. a massless quark needs $\gtrsim$ 2.5 GeV of energy against the c.m. to be able to form a jet. For gluons the jet threshold certainly is not lower. But a gluon carries the colour indices of a quark antiquark pair and each index may fragment separately. Then the multiplicity of the jet may be higher and the longitudinal hadron momenta may be lower. In the limit of asymptotic energies the gluon may just fragment like a $q\bar{q}$ pair, each quark carrying half the gluon momentum [55]. From this picture follows that a gluon jet of a certain longitudinal momentum will have a higher multiplicity and a larger opening angle than a quark jet of the same momentum. The threshold for gluon jet production will be higher than that for quark jet production with an upper bound of two times the quark threshold [+].

Some possible sources of gluon jets are shown in Fig. 7.3, the pseudoscalars

[+] Speaking of a jet threshold we refer to the energy of a single quark or gluon versus the center of mass of the colour bag.

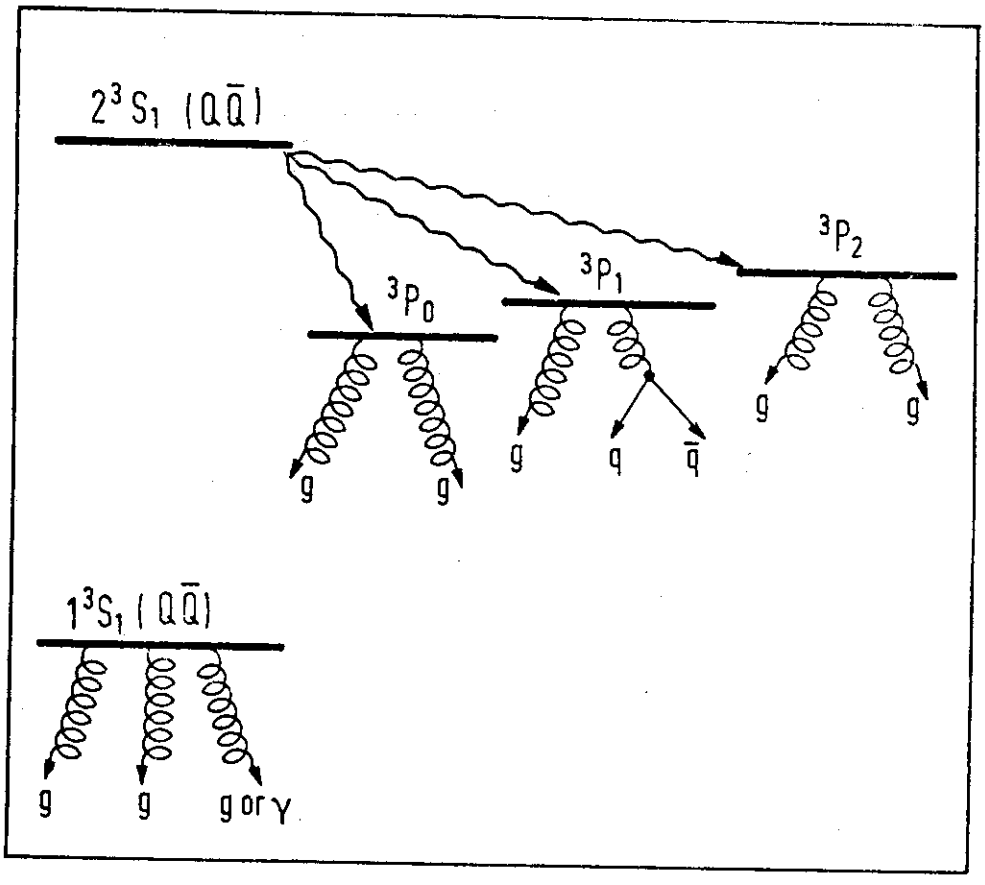

Fig. 7.3. Possible sources of gluon jets in heavy Quarkonia.

are omitted, they may also form 2 jets out of the 2 decay gluons. We begin with the $^3S_1$ decay into 3 gluons. The three gluons of this decay will form a plane. The angular distribution of the normal $\hat{n}$ of this plane against the beam is

$$\frac{d\Gamma}{d\cos\theta_{\hat{n}e}} \sim 3 - \cos^2\theta_{\hat{n}e} \qquad (7.1)$$

For these decays one defines a variable T "Thrust", which is just the scaled energy of the most energetic gluon, $T = x_1 = 2p_{g_1}/M_{Q\bar{Q}}$. The direction of g_1 defines the Thrust axis. The differential rate of the 3 gluon decay together with the angular distribution of this Thrust axis is shown in Fig. 7.4. While off resonance the coefficient of the $\cos^2$ term, α , is uniquely 1, it shows a T dependence for $Q\bar{Q}$ decays. The average of $\alpha(T)$ for $Q\bar{Q} \rightarrow 3g$ is 0.39. A much more detailed discussion is given in Ref. 56).

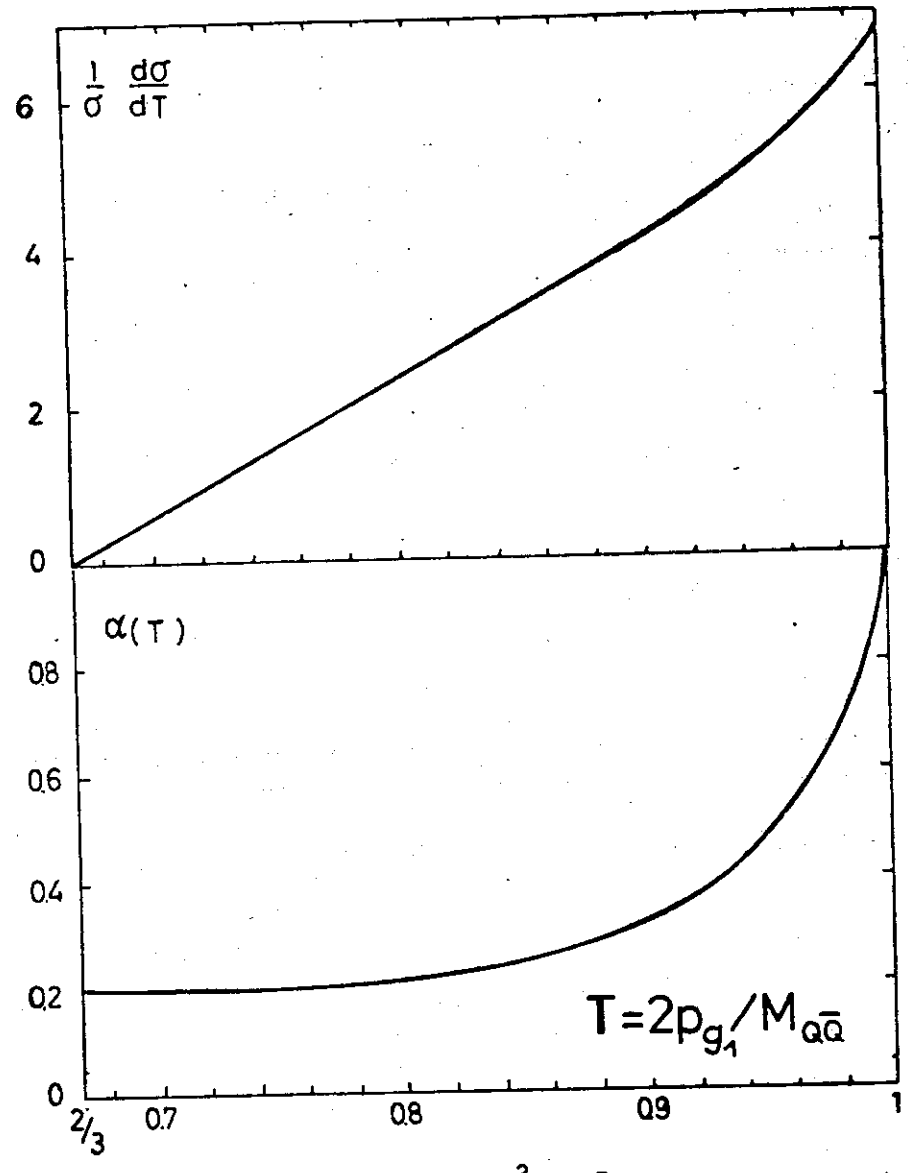

Fig. 7.4. The differential rate of $^3S_1(Q\bar{Q}) \rightarrow 3g$ and the thrust angular distribution $W \sim 1 + \alpha(T) \cos^2\theta_{Te}$ as functions of T. θ_{Te} is the angle between the thrust axis and the beam.

Once the 3 gluon jet decay and the γ+ 2 gluon jet decay is found, we can start to compare deviations from the lowest order angular distributions, which arise through <u>different</u> interactions between two gluon jets, Fig. 7.5. The lowest order (Born-approximation) graph gives for the opening angle of the second and third energetic gluon θ_{23} (compare Fig. 7.6) the distribution displayed in Fig. 7.7. The deviations from this distribution will be different in case a) and b) of Fig. 7.5 because in case a) the interaction

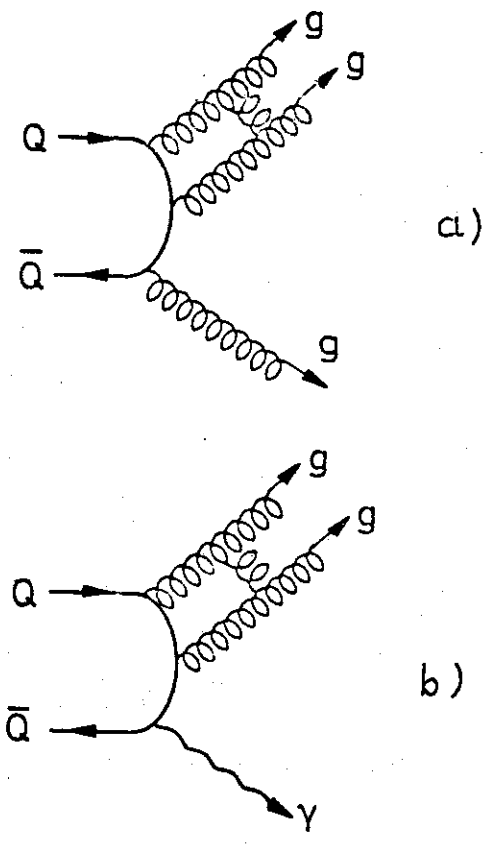

Fig. 7.5. Possible next order ($\frac{\alpha_s}{\pi}$) interactions between gluon jets.

between the two gluon jets happens in a colour octet (they should repel) whereas in case b) it is in a colour singlet (they should attract).

We will remain at the $\gamma 2g$ decay for another while. The kinematics of this process differ from the 3g decay because the γ can be identified for all photon momenta between 0 and $M_{Q\bar{Q}}/2$. The distributions corresponding to Fig. 7.4 are given in Fig. 7.8. One notices that the angular correlation drops very fast to a minimum if one goes away from the kinematical limit $E_\gamma = M_{Q\bar{Q}}/2$. For the limit $E_\gamma = 1/2\ M_{Q\bar{Q}}$ the coefficient α in front of the $\cos^2\theta$ term is + 1. This is easy to understand. In this limit the two gluons have to go parallel. Their helicities (transverse polarisation) have to add up to either 0 or $\pm$ 2 (For scalar gluons it is 0). Since the photon on the other side is also transverse, the decaying helicity state is the $\lambda = \pm 1$ state. This leads to $1 + \cos^2\theta$. One can show further, that the helicities of the parallel gluons are opposite. If we give the gluon pair a small angle, the net helicity remains zero most of the time. But now we can Lorentz transform to the c.m.s. of the gluon pair and find $\lambda_{cms} = \pm 2$! This means: If low mass hadrons are produced in the process $Q\bar{Q} \rightarrow \gamma + 2g \rightarrow \gamma +$ hadron, the gluon mechanism favours spin ≥ 2 hadrons over spin 1 or spin 0 hadrons. By this spin argument we can understand the rate for $J/\psi \rightarrow \gamma f$, which is of the same magnitude as $J/\psi \rightarrow \gamma\eta$ and $\gamma\eta'$ although the η and η' should couple

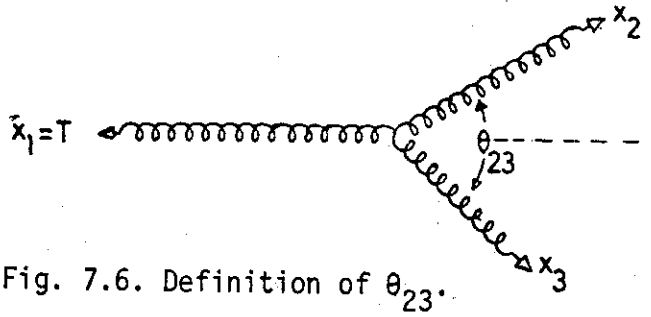

Fig. 7.6. Definition of θ_{23}.

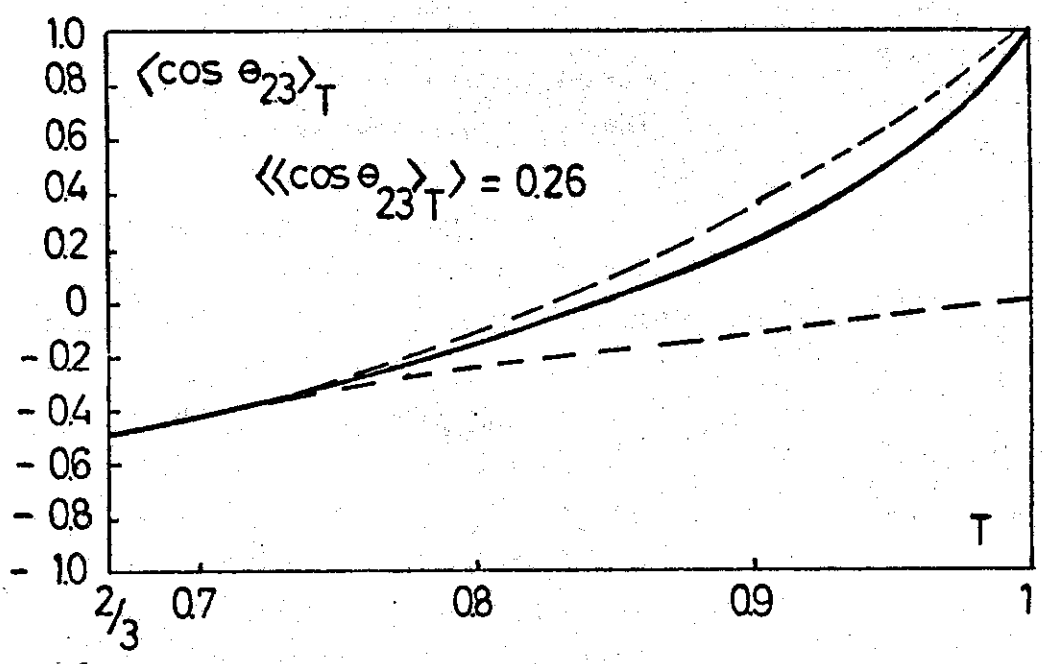

Fig. 7.7. The mean value of θ_{23}, as defined in Fig. 7.6. as a function of T. The dashed lines show the kinematic boundaries.

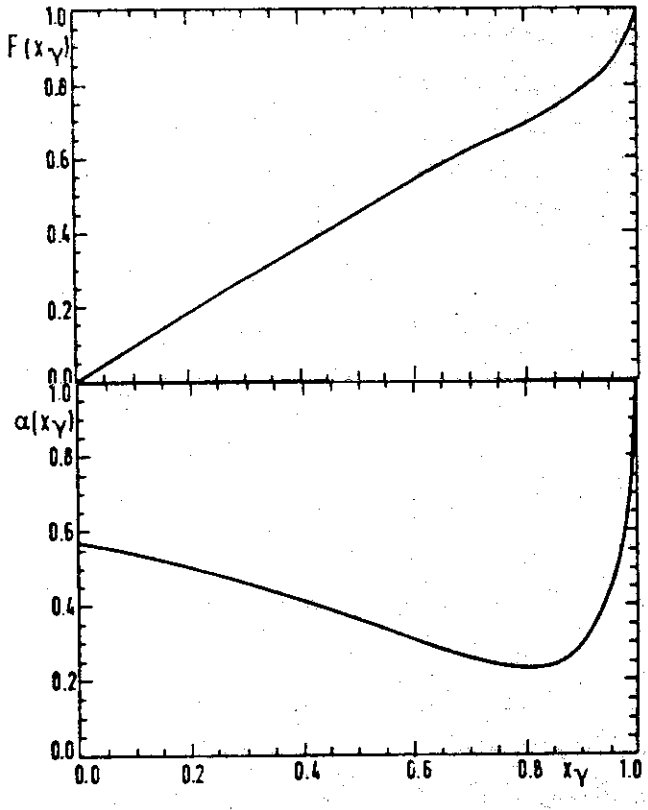

Fig. 7.8. Differential rate $F(x_\gamma) = \frac{d\Gamma}{dx_\gamma}$ and angular distribution $1+\alpha(x_\gamma)\cos^2\theta_{fe}$ as a function of $x_\gamma = 2E_\gamma / M_{Q\bar{Q}}$

to two gluons much stronger because of their large violation of the Zweig rule. The whole argument can of course be made quantitative. The ratios of the helicity amplitudes for $1^{--}(^3S_1) \to \gamma^* + gg \to \gamma^* + 2^{++}(^3P_2)$ will depend on the two gluon (or hadron) mass. This is shown in Fig. 7.9 [57]. At the point, $J/\Psi \to \gamma f$, these ratios have been measured and agree with this QCD estimate, see Fig. 7.10. They also agree with the tensor meson dominance (TMD) model studied here at Karlsruhe [58].

From our short excursion we now return to two jets from P wave decays. The first P wave of Quarkonium can be reached from the first

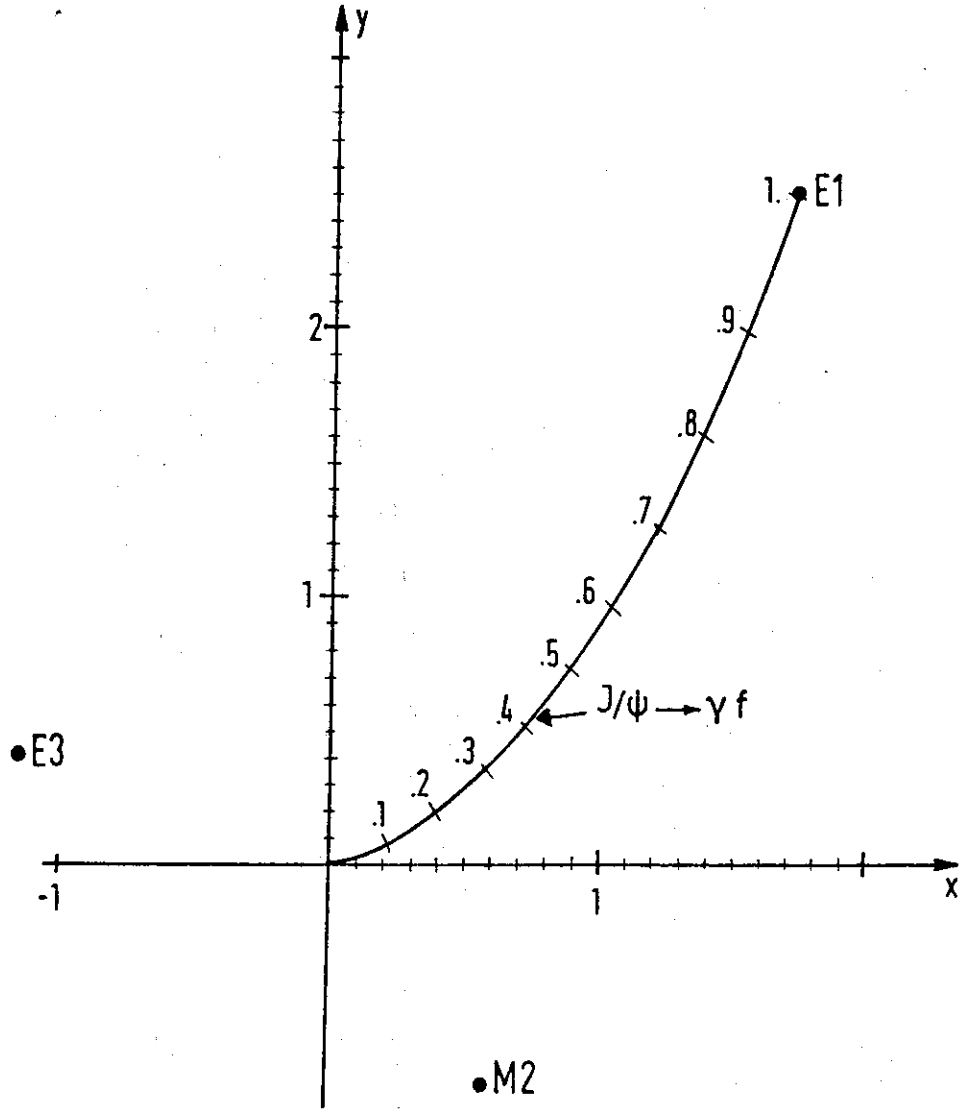

Fig. 7.9. Helicity amplitudes in $^3S_1(Q\bar{Q}) \rightarrow \gamma + {}^3P_2(q\bar{q})$ as a function of $M(^3P_2)/M(Q\bar{Q})$. The $A_{|i|}$ are helicity amplitudes. E1, M2, E3 denote the familiar multipole transitions, the (x,y) pair for $J/\psi \rightarrow \gamma f$ is indicated. $x = A_1/A_0$, $y = A_2/A_0$.

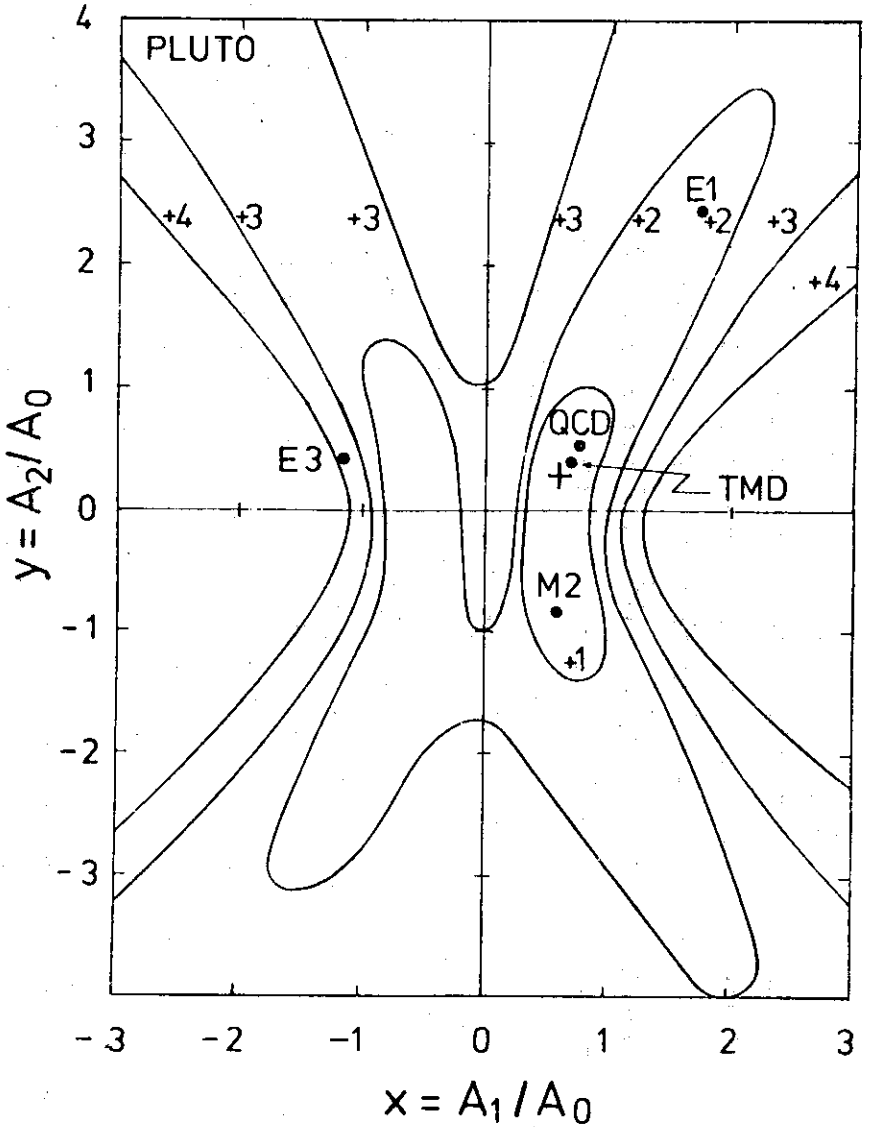

Fig. 7.10. A measurement of the predicted (x,y) pair of Fig. 7.9 for $J/\psi \rightarrow \gamma f$ by the PLUTO collaboration. The cross is the central value of the experiment, the lines indicate standard deviations.

radially excited S wave, e.g. Υ', via an E1 transition. Experimentally it will be necessary to trigger on this monochromatic photon to identify the P wave. The P state then can decay into 2 gluons in case of the $^3P_0$ and $^3P_2$ states. We will discuss the jet decay of the $^3P_1$ state later. These two gluons have a distinct energy of half the P state mass. This is the essential difference to the 3 jet decay of Quarkonium. Here we have monochromatic jets! In Υ' the jet energy is almost 5 GeV, this should be sufficient to determine the original gluon direction via the jet direction. A measurement of the gluon angular distributions becomes feasible! For the decay of the $^3P_0$ state this angular distribution is trivial: no matter, what the dynamics are, there is only one helicity amplitude which can contribute. But in the $^3P_2$ decays there are two independent helicity amplitudes for massless gluons. The QCD matrix element for the $^3P_2 \to gg$ decay reads with $q \equiv k_1 - k_2$

$$\epsilon_{\mu\nu}(\lambda)\left[4\, k_1\cdot k_2\, \varepsilon_1^{*\mu}\varepsilon_2^{*\nu} - \varepsilon_1^{*}\cdot\varepsilon_2^{*}\, q^\mu q^\nu + 2k_1\cdot\varepsilon_2^{*}\,\varepsilon_1^{*\mu} q^\nu - 2k_2\cdot\varepsilon_1^{*}\,\varepsilon_2^{*\mu} q^\nu\right] \qquad (7.2)$$

and it turns out that the decay is in the helicity $\lambda = \pm 2$ state. Eq. (7.2) with $\epsilon_{\mu\nu}(o)$ just vanishes for transverse $\varepsilon_1, \varepsilon_2$. The formula for the kinematics gives us, integrated, the distribution

$$W_{2g}^{2^{++}}(\theta_{\gamma j}) \sim 1 + \cos^2\theta_{\gamma j} \qquad (7.3)$$

where $\theta_{\gamma j}$ is the angle between the trigger photon and one of the jets, measured in the c.m.s. of the jets (Fig. 7.11). If the $^3P_2$ would decay into

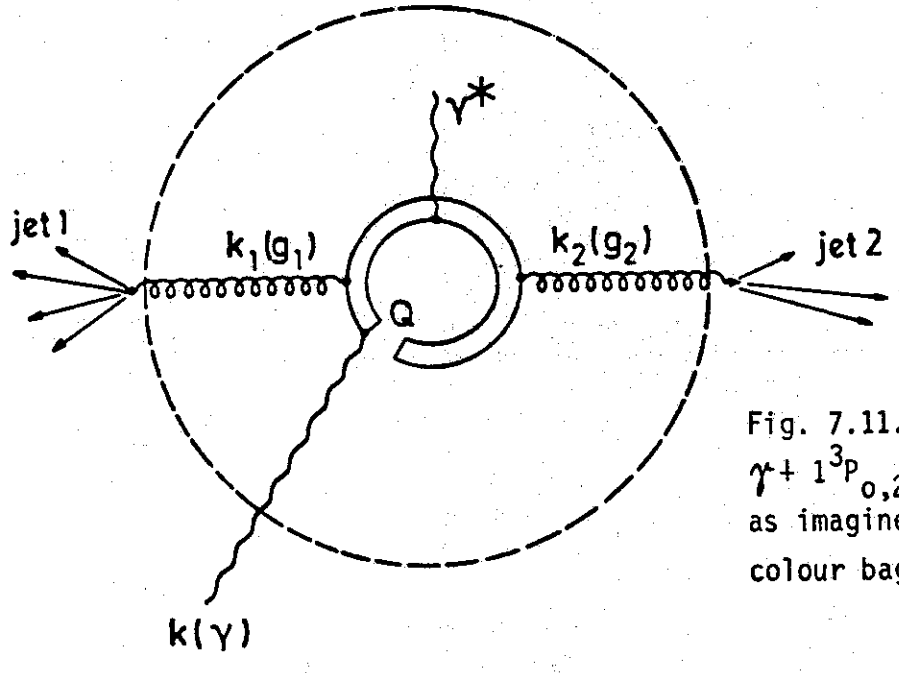

Fig. 7.11. $2^3S_1(Q\bar{Q}) \longrightarrow \gamma + 1^3P_{0,2}(Q\bar{Q}) \to \gamma +$ 2 g jets, as imagined within the colour bag.

two quark jets by some arbitrary mechanism, the helicity of the two quarks can at most add up to $\lambda = \pm 1$. The kinematic formula then gives

$$W^{2^{++}}_{q\bar{q}}(\theta_{\gamma j}) \sim 1 - \frac{6+3A^2}{10+9A^2}\cos^2\theta_{\gamma j}\ , \qquad (7.4)$$

where A gives the weight of helicities $\lambda = \pm 1$ over helicity 0. The sign difference between (7.4) and (7.3) allows a clear test of the QCD mechanism. The rate for this process will be around 5 % of all Υ'decays [15].

As we have discussed in Chapter 6) the $^3P_1$ decay proceeds via the complicated graph c) of Fig. 6.4. The decay is displayed again in Fig. 7.12.

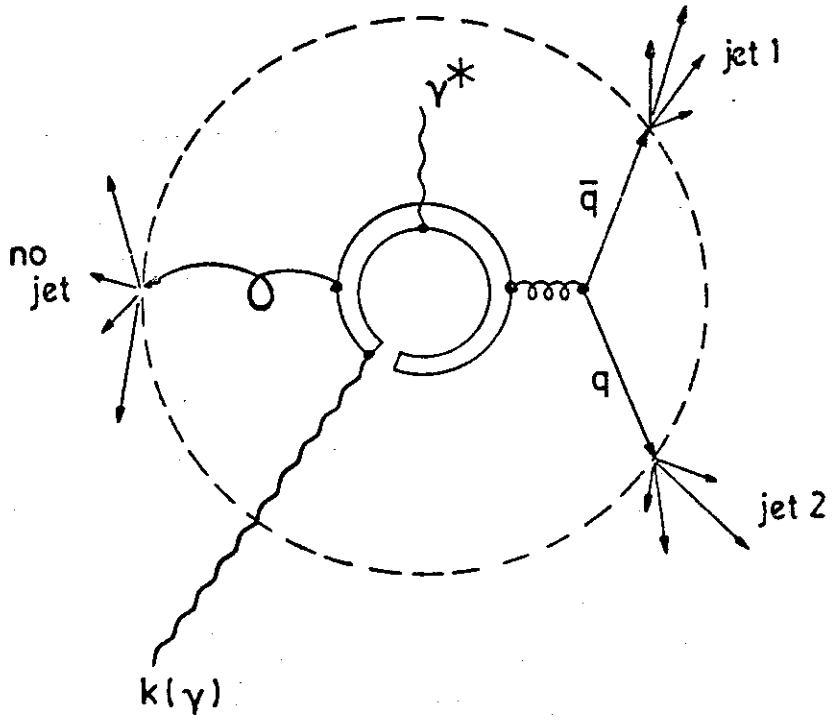

Fig. 7.12. $2^3S_1(Q\bar{Q}) \to \gamma + 1^3P_1(Q\bar{Q}) \to \gamma$ + 2 quark jets. Here a soft gluon recoils against the two quark jets.

We will see two quark jets and a hadron cloud from the soft gluon from this decay. The quark jets should be easy to detect. Their angular distribution is given by

$$W^{1^{++}}_{gq\bar{q}} \sim 2 - \cos^2\theta_{\gamma e} + \cos\theta_{\gamma e}\cos\theta_{\gamma j}\cos\theta_{je}\ , \qquad (7.5)$$

already smeared over the important kinematic regime of small gluon momentum [50,59]. $\theta_{\gamma j}$ is the same angle as before, $\theta_{\gamma e}$ is the angle between the trigger photon and the beam, say e^-, and θ_{je} is the angle between the same jet arm as for $\theta_{\gamma j}$ and e^-. $\theta_{\gamma e}$ is measured in the lab frame, but θ_{je} as well as $\theta_{\gamma j}$ are in the c.m.s. of the jets. As an alternative process, the decay into two massless quarks would give [59]

$$W_{q\bar{q}}^{1^{++}} \sim 1 - \cos\theta_{\gamma e} \cos\theta_{\gamma j} \cos\theta_{je} \quad . \tag{7.6}$$

Here the $\cos^2\theta_{\gamma e}$ term is missing and the term linear in the cosines has a different sign. But the most important difference between the two alternatives (7.5) and (7.6) is the recoil of the soft gluon in the $gq\bar{q}$ decay of the $^3P_1$ state. This recoil will be much larger than the recoil of the trigger photon alone which of course is always present. But with the recoil of the trigger photon alone, the 2 jets would be collinear up to a 10^0 deviation at most. From the recoil of the soft gluon in the decay of the $^3P_1$ state, however, the angle between the two quark jets may be as small as 110^0. This is true for the Υ system. For a heavier Quarkonium the "soft" gluon may even form a third jet in a small subset of all events.

8. Conclusions

The simplest ansatz for the $Q\bar{Q}$ potential, which is possible using the hints from QCD, works astonishingly well. The short distance spin dependent part of the potential describes the spin orbit splittings reasonably well! If it is correct, heavier Quarkonia should show i) a decrease of the LS splittings $\sim 1/m_Q$ roughly, ii) a tendency of $R = \frac{M(2^{++}) - M(1^{++})}{M(1^{++}) - M(0^{++})} \to 0.8$ from 0.5 in $c\bar{c}$. The confinement part of the potential may be spin-independent, as suggested by lattice gauge theories. Its strength depends on the ansatz for the potential at intermediate distances, it is, however, very close to the value suggested by the higher orbital excitations of light mesons (Regge slope). Many details depend on the proper choice for the intermediate distance potential. QCD gives us no hint here. To speculate a little, level spacings might remain almost the same for the next Quarkonium while $\Gamma_{e\bar{e}}/e_Q^2$ might increase very slightly. The number of narrow (=bound) states below the new flavour threshold will increase for the next Quarkonia. Υ''' might turn out as a perfect B meson factory ($M(\Upsilon''') \simeq 10.6$ GeV).

We seem to understand parity changing photon transitions in terms of E1 radiation. This means that we understand the "size" of Charmonium. We also seem to understand the branching fractions of P wave decays via the special QCD annihilation mechanism into gluons. This is a short distance phenomenon. We further seem to understand the relative magnitude of $J/\psi \to \gamma f$ and $\gamma\eta$ via a simple gluon spin argument.

Up to now we do not know <u>any</u> Quarkonium pseudoscalar state definitely. The experimental candidates $X(2.83), \chi(3.45), \chi(^{3.59}_{3.18})$ cannot be understood in terms of QCD. Especially their M1 transitions and gluon annihilation properties should be much different from what is observed for these states.

Our hopes for the future are that gluon jets show up. Then we can measure the gluon spin and verify certain QCD processes like $^3P_1 \to gq\bar{q}$. In the $^3S_1$ decay we can study the gluon selfinteraction by comparing γgg vs. $3g$ decays. Finding the gluons is most interesting and important, since they are the gauge bosons of the supposed nonabelian gauge theory of strong interactions, QCD, as the $W^{\pm}$, Z, and γ in weak and electromagnetic interactions.

References

1) J.J. Aubert et al., Phys. Rev. Lett. 33 (1974) 1404;
J.E. Augustin et al., Phys. Rev. Lett. 33 (1974) 1406;
G.S. Abrams et al., Phys. Rev. Lett. 33 (1974) 1453;
For reviews see:
B.H. Wiik and G. Wolf, DESY 78/23 (May 1978);
G.J. Feldman and M.L. Perl, Phys. Rep. 33C (1977) 285.

2) M. Gell-Mann, Phys. Lett. 8 (1964) 214;
G. Zweig, CERN Preprints TH 401, 412 (1964).

3) J.D. Bjorken and S.L. Glashow, Phys. Lett. 11 (1964) 255;
S.L. Glashow, J. Iliopoulos and L. Maiani, Phys. Rev. D2 (1970) 1285;
M.K. Gaillard, B.W. Lee and J.L. Rosner, Rev. Mod. Phys. 47 (1975) 277.

4) T. Appelquist and H.D. Politzer, Phys. Rev. Lett. 34 (1975) 43;
A. De Rújula and S.L. Glashow, Phys. Rev. Lett. 34 (1975) 46;
T. Appelquist et al., Phys. Rev. Lett. 34 (1975) 365;
E. Eichten et al., Phys. Rev. Lett. 34 (1975) 369.

5) S.W. Herb et al., Phys. Rev. Lett. 39 (1977) 252;
W.R. Innes et al.; Phys. Rev. Lett. 39 (1977) 1240;
Ch. Berger et al., Phys. Lett. 76B (1978) 243;
C.W. Darden et al., Phys. Lett. 76B (1978) 246;
J.K. Bienlein et al., Phys. Lett. 78B (1978) 360;
C.W. Darden et al., Phys. Lett. 78B (1978) 364.

6) M. Kobayashi and K. Maskawa, Progr. Theor. Phys. 49 (1973) 652;
Y. Achiman, K. Koller and T.F. Walsh, Phys. Lett. 59B (1975) 261;
For a review see:
J. Ellis et al., Nucl. Phys. B131 (1977) 285.

7) H. Fritzsch, M. Gell-Mann and H. Leutwyler, Phys. Lett. B47 (1973) 365;
D.J. Gross and F. Wilczek, Phys. Rev. D8 (1973) 3497;
S. Weinberg, Phys. Rev. Lett. 31 (1973) 494.

8) G. 't Hooft, unpublished;
D.J. Gross and F. Wilczek, Phys. Rev. Lett. 30 (1973) 1343;
H.D. Politzer, Phys. Rev. Lett. 30 (1973) 1346.

9) K.G. Wilson, Phys. Rev. D10 (1974) 2445;
J. Kogut and L. Susskind, Phys. Rev. D11 (1975) 395;
For a review see:
H. Joos, in "Proc. of the International Summer Institute on Theoretical Particle Physics in Hamburg 1975" (J.G. Körner et al., eds. , Springer, Berlin, 1976) and DESY 76/36 (July 1976).

10) H. Nielsen and P. Olesen, Nucl. Phys. B61 (1973) 45;
J. Kogut and L. Susskind, Phys. Rev. D9 (1973) 2273;
Y. Nambu, Phys. Rev. D10 (1974) 4262;
B. Brout, F. Englert and W. Fischler, Phys. Rev. Lett. 36 (1975) 649;
For a review see:
M. Böhm and H. Joos, DESY 78/27 (May 1978).

11) V.B. Berestetski, Sov. Phys. Uspekhi 19 (1976) 934.

12) W. Celmaster, H. Georgi and M. Machacek, Phys. Rev. D17 (1978) 879.

13) L.D. Landau and E.M. Lifshitz, Relativistic Quantum Theory (Pergamon Press, 1971); A.I. Achieser and W.B. Berestezki, Quantenelektrodynamik (Teubner, Leipzig, 1962); J. Pumplin, W. Repko and A. Sato, Phys. Rev. Lett. 35 (1975) 1538 and references therein; D. Gromes, Nucl. Phys. B131 (1977) 80.

14) J. Ellis, M.K. Gaillard and G.G. Ross, Nucl. Phys. B111 (1976) 253; T.A. DeGrand, Y.J. Ng and S.H.H. Tye, Phys. Rev. D16 (1977) 3251; K. Koller and T.F. Walsh, Phys. Lett. 72B (1977) 227 and 73B (1978) 504; S.J. Brodsky, D.G. Coyne, T.A. DeGrand and R.R. Horgan, Phys. Lett.73B (1978) 203; H. Fritzsch and K.H. Streng, Phys. Lett. 74B (1978) 90; K. Hagiwara, Nucl. Phys. B137 (1978) 164; A. De Rújula et al., Nucl. Phys. B138 (1978) 387; K. Koller and T.F. Walsh, Nucl. Phys. B140 (1978) 449; K. Koller, H. Krasemann and T.F. Walsh, DESY 78/37 (1978).

15) M. Krammer and H. Krasemann, Phys. Lett. 73B (1978) 58; H. Krasemann, DESY 78/46 (Sept. 1978), to appear in "Zeitschrift für Physik C".

16) D. Robson, Nucl. Phys. B130 (1977) 328 and references therein; P. Roy and T.F. Walsh, Phys. Lett. 78B (1978) 62.

17) See the lectures by F. Dydak and W. Williams, this school.

18) E. Eichten and K. Gottfried, Phys. Lett. 66B (1977) 286.

19) C. Quigg and J.L. Rosner, Phys. Lett. 71B (1977) 153.

20) G. Bhanot and S. Rudaz, Phys. Lett. 78B (1978) 119.

21) E. Eichten et al., Phys. Rev. D17 (1978) 3090.

22) For a derivation on the classical level see the text books, e.g. A. Sommerfeld, Atombau und Spektrallinien (Vieweg, Braunschweig, 1950) or J.D. Jackson, Classical Electrodynamics (J. Wiley and Sons, New York 1962). In the framework of the Bethe Salpeter equation for Charmonium see A.B. Henriques, B.H. Kellett and R.G. Moorhouse, Phys. Lett. 64B (1976) 85.

23) G. Buschhorn, this school.

24) See e.g.: A.I. Achieser and W.B. Berestezki, ref. 13, § 39.

25) F. Wilczek and A. Zee, Phys. Rev. Lett. 40 (1978) 83.

26) H.J. Schnitzer, Phys. Lett. 65B (1976) 239.

27) R. Barbieri, R. Gatto, R. Kögerler and Z. Kunszt, Phys. Lett. 57B (1975) 455.

28) J.L. Rosner, C. Quigg and H.B. Thacker, Phys. Lett. 74B (1978) 350.

29) C. Quigg and J.L. Rosner, Phys. Lett. 72B (1978) 462.

30) P. Ditsas, N.A. McDougall and R.G. Moorhouse, Glasgow preprint (1978).

31) See the text books, e.g. W. Heitler, The Quantum Theory of Radiation (Oxford Univ. Press, London, 1947),
J.M. Blatt and V.F. Weisskopf, Theoretical Nuclear Physics (J. Wiley and Sons, New York, 1952), or
S.A. Moszkowski in Beta and Gamma Ray Spectroscopy, K. Siegbahn ed. (North Holland, Amsterdam, 1955).

32) L.B. Okun and M.B. Voloshin, preprint ITEP 152 (Moscow 1976);
V.A. Novikov et al., Phys. Rep. 41C (1978) 1.

33) H. Krasemann, Thesis, Hamburg 1978.

34) J.D. Jackson, Phys. Rev. Lett. 37 (1976) 1107;
H.A. Bethe and E.E. Salpeter, Quantum Mechanics of One- and Two-Electron Atoms, Springer Verlag (Berlin, Göttingen, Heidelberg, 1957).

35) See e.g.: Bethe and Salpeter, ref. 34.

36) W. Bartel et al., DESY 78/49 (September 1978);
see also the lecture of Prof. Buschhorn at this school.

37) A. De Rújula, in "Current Induced Reactions", Int. Summer Institute on Theoretical Particle Physics in Hamburg 1975 (Springer Verlag, Eds. J.G. Körner, G. Kramer and D. Schildknecht).

38) K. Gottfried, in "Proc. 1977 International Symposium on Lepton and Photon Interactions at High Energies" (DESY, F. Gutbrod ed.).

39) R.L. Jaffe, in "Quark Spectroscopy and Hadron Dynamics", Proc. of Summer Institute on Particle Physics, 1977 (SLAC, M.C. Zipf ed.).

40) K. Gottfried, Phys. Rev. Lett. 40 (1978) 598 and ref. 38.

41) T. Appelquist and H.D. Politzer, Phys. Rev. D12 (1975) 1404.

42) H. Pietschmann and W. Thirring, Phys. Lett. 21 (1966) 713;
R. Van Royen and V.F. Weisskopf, Nuovo Cim. 50 (1967) 617;
ibid. 51 (1967) 583.

43) A. Ore and J.L. Powell, Phys. Rev. 75 (1949) 1696.

44) These conversion factors are reviewed in ref. 32.

45) I. Ya. Pomeranchuk, Doklady Akademii Nauk SSSR 60 (1948) 263.

46) A.I. Alekseev, Sov. Phys. JETP 34 (1958) 826.

47) R. Barbieri, R. Gatto and R. Kögerler, Phys. Lett. 60B (1976) 183.

48) C.N. Yang, Phys. Rev. 77 (1950) 242; compare also L.D. Landau and E.M. Lifshitz, ref. 13.

49) R. Barbieri, R. Gatto and E. Remiddi, Phys. Lett. 61B (1976) 465.

50) H. Krasemann, ref. 15.

51) W. Braunschweig et al., Phys. Lett. 67B (1977) 243;
W. Bartel et al., Phys. Lett. 64B (1976) 483;
G. Alexander et al., Phys. Lett. 72B (1978) 493;
R. Brandelik et al., Phys. Lett. 76B (1978) 361.

52) DASP-II-Collaboration, Internal Report DESY F15-78/01 (August 1978).

53) R.F. Schwitters et al., Phys. Rev. Lett. 35 (1975) 1320;
G. Hanson et al., Phys. Rev. Lett. 35 (1975) 1609;
G. Hanson, SLAC PUB 2118 (1978);
PLUTO-Collaboration, Phys. Lett. 78B (1978) 176.

54) J. Ellis, M.K. Gaillard and G.G. Ross, ref. 14.

55) K. Koller and T.F. Walsh, ref. 14.

56) K. Koller, H. Krasemann and T.F. Walsh, ref. 14.

57) M. Krammer, Phys. Lett. 74B (1978) 361.

58) W. Gampp and H. Genz, Phys. Lett. 76B (1978) 319.

59) A. De Rújula et al., ref. 14.